Deuteron NMR and Spin-Lattice Relaxation Studies of a Manganese-Ion Cluster Nanomagnet

Achey, R.M., NHMFL/FSU, Chemistry
Dalal, N.S., NHMFL/FSU, Chemistry
Arcon, D., J. Stefan Institute, Ljubljana, Slovenia
Dolinsek, J., J. Stefan Institute, Ljubljana, Slovenia
Apih, T., J. Stefan Institute, Ljubljana, Slovenia
Blinc, R., J. Stefan Institute, Ljubljana, Slovenia
Vonlanthen, P., Laboratorium fur Festkorperphysik, ETH Honggerberg, Zurich, Switzerland
Gavilano, J.L., Laboratorium fur Festkorperphysik, ETH Honggerberg, Zurich, Switzerland
Ott, H.R., Laboratorium fur Festkorperphysik, ETH Honggerberg, Zurich, Switzerland

Structural studies of molecule-based magnetic clusters have recently attracted attention because they allow for a study of the transition from molecular paramagnetism to bulk ferromagnetism.[1,2] Here we summarize our deuteron NMR and spin-lattice relaxation study of fully deuterated Manganese-12 Acetate $[Mn_{12}O_{12}(CD_3COO)_{16}(D_2O)_4]\cdot 2CD_3COOD \cdot 4D_2O$ (abbreviated as d-$Mn_{12}O_{12}$), where superparamagnetic properties have been recently discovered. This summary is based on our two recent preliminary reports.[3,4]

The ground state configuration of this system is determined by the antiferromagnetic superexchange interactions through the bridging oxygens between the four inner Mn^{4+} (S=3/2) and the eight outer Mn^{3+} (S=2) ions. The ferromagnetic (S=10) ground state is established if all the Mn^{3+} spins are "up," and all the Mn^{4+} spins are "down". For a better understanding of the ground state configuration it is important to know whether there is any spin density delocalization over the organic ligands. For that purpose NMR is the direct method of choice. Given that the spin density is delocalized, the deuteron spin-lattice relaxation rate thus measures the spectral density of the fluctuations in the electronic spin-deuteron hyperfine couplings at the Larmor frequency of the measurements, here 41.46 MHz in a field of 6.34 T. These measurements on d-$Mn_{12}O_{12}$ show that the relaxation is due to fluctuations in the electron-nuclear hyperfine interaction. The temperature dependence of T_1 showed two pronounced minima, around 70 K and 10 K. The correlation time for the slower relaxation mode is of the order of days in the vicinity of the superparamagnetic blocking temperature, while the faster correlation time is still in the microsecond range at that temperature.

This study shows that the unpaired electron spin density extends over the whole Mn ion cluster, rather than being localized at the core of the cluster. This result, and the fact that fluctuations in the electron-nuclear hyperfine coupling determine the deuteron T_1, agrees with the neutron diffraction data in an applied field. The two relaxation modes detected in this study are in the intermediate frequency range between the slow magnetic reorientation mode detected by ac susceptibility data, and the fast spin modes detected by inelastic neutron scattering. Further analysis of the data obtained is in progress.

References:

1 Awschalom, D.D., *et al.*, Science, 258, 414 (1992).
2 Sessoli, R., *et al.*, Nature (London), 365, 141 (1993).
3 Dolinsek, J., *et al.*, Europhys. Lett., 42, 6, 691 (1998).
4 Arcon, D., *et al.*, Phys. Rev. B, 58, 6, R2941 (1998).

Magnetic Interactions and Evidence for the Two Sublattice Model of $Mn_{12}O_{12}$ Acetate by ^{13}C NMR Spectroscopy

NHMFL

Achey, R.M., NHMFL/FSU, Chemistry
Reyes, A.P., NHMFL
Kuhns, P.L., NHMFL
Moulton, W.G., NHMFL/FSU, Physics
Dalal, N.S., NHMFL/FSU, Chemistry

Manganese Acetate is perhaps the first single crystal system that exhibits quantum tunneling of magnetization (QTM). An important question is whether electronic spin density is concentrated on the 12-Mn cluster, or distributed on the entire molecular framework.. The ^{13}C spectrum of ^{13}C $Mn_{12}O_{12}$ at 296 K at 151.7 MHz for an aligned sample with H||c is shown in the inset of Figure 1.

The spectrum shows the methyl group ^{13}C nuclei experience four different local hyperfine fields. The peaks are labeled A, B, C, and D. We assign the A peak to the methyl groups that are oriented perpendicular to the ring, i.e., the direction along which we expect the internal field to be oriented. We assign peak B to the CH_3 carbons of the acetate groups whose oxygens bridge one Mn^{3+} ion of the outer ring and one Mn^{4+} ion from the inner tetrahedron. This is because the coupling between the two Mn ions is antiferromagnetic and thus the resultant hyperfine field is much smaller than the ferromagnetic coupling between two Mn^{3+} ions. Peak D is assigned to the eight CH_3 groups oriented in the plane of the ring, based on the fact that the shift is of significantly smaller magnitude and of opposite sign to that of peak A. The shift is a linear function of magnetization at high temperature but deviates below 100 K, where the system seems to enter another magnetic regime. The nature of this transition is not yet clear; and T_1 studies of the dynamics are underway. The hyperfine fields are 0.235, 0.138, and -0.077 kOe/μ_B for peaks A, B, and D respectively. A dipole calculation gave results consistent with these assignments. The observation of four distinct peaks, and their relative magnitude and signs are consistent with the two-sublattice model.

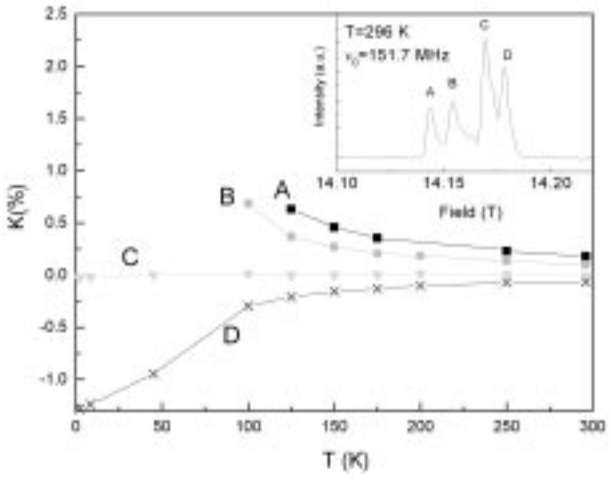

Figure 1. Shift as a function of temperature for peaks shown in the inset room temperature spectrum.

This work is supported by the NHMFL In-House Research Program.

ESR Study of (Mg, Zn) Doped $CuGeO_3$

NHMFL

Biskup, N., NHMFL
Brooks, J.S., NHMFL/FSU, Physics
Jackson, D., NHMFL
Fisk, Z., NHMFL/FSU, Physics
Dalal, N., NHMFL/FSU, Chemistry

$CuGeO_3$ is, as a first inorganic compound exhibiting spin-Peierls transition, investigated intensively since its discovery in 1993.[1] The possibility of doping (Zn, Mg) makes it even more suitable for studies of magnetic ordering. The ESR absorption reveals angular anisotropy with highest g-factor in B || b direction ($g \approx 2.2$). The intensity shows a sharp drop below spin-Peierls transition temperature T_{SP} = 14 K, which can be reasonably well adjusted to the theoretical form of an alternating spin chain. In doped samples, additional

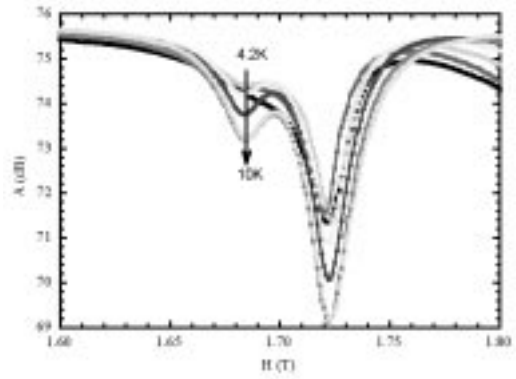

Figure 1. ESR absorption lines of $Cu_{0.99}Mg_{0.01}GeO_3$ for a set of temperatures.

peaks were reported coming from the broken chains due to impurities. We performed initial measurements of ESR absorption in a series of monocrystals of pure and doped material. A millimeter wave vector analyzer (MVNA) was configured to monitor the absorption of mm-range radiation (40 GHz to 100 GHz). The radiation absorption is obtained in a resonant cavity with a Q factor of up to 20,000, which enables high sensitivity. The ESR spectrum of the $Cu_{0.99}Mg_{0.01}GeO_3$ sample is shown in Figure 1. Besides a regular, pure $CuGeO_3$ ESR peak, an additional starts to emerge above 4 K to 5 K for both Mg and Zn doped samples. Although the temperature dependence of the ESR intensity seems to follow the same activated decrease below T_{SP} (Figure 2), the low temperature behavior is different. It appears that the second peak (lower B) disappear at approximately 5 K, while the intensity of the first increase. This is unexpected from the simple model mentioned above. However, it is worth to note that the low-T increase of amplitude coincide with the onset of additional antiferromagnetic ordering (Néel temperature) recently reported in doped crystals.[2]

References:

1 Boucher, J.P., *et al*., J. Phys. 1, France 6, 1939 (1996).
2 Hase, M., *et al*., Phys. Rev. B, 54, 3722 (1996).

High Frequency Splitting of ESR Peaks in K_3CrO_8

NHMFL

Biskup, N., NHMFL
Brooks, J.S., NHMFL/FSU, Physics
Dalal, N., NHMFL/FSU, Chemistry

Detailed theoretical analyses of simple Heisenberg chain systems are usually hindered by the presence of hyperfine and/or zero field (dipolar) coupling terms in the spin Hamiltonian. The Cr (5+) -3d1 salt K_3CrO_8 can serve as the simplest case a new model system for investigating the chain dynamics, and possible magnetic exciton formation and trapping in such systems.[1] We have carried out detailed ESR measurements on single crystals of K_3CrO_8 over the frequency ranges of 40 GHz to 101 GHz, and temperatures from 1.2 K to 60 K. While single absorption line is observed for frequencies lower than 60 GHz, the splitting occurs at higher frequencies. The example of these splitting

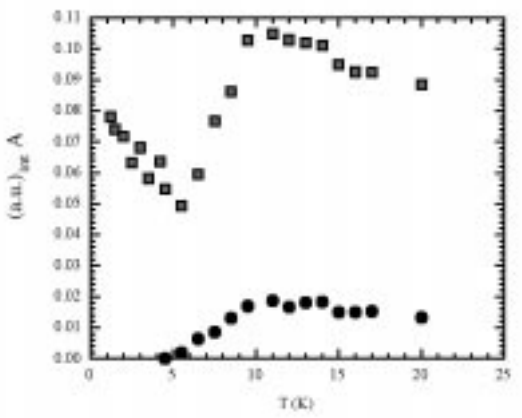

Figure 2. Temperature dependence of amplitude of two peaks in Figure 1.

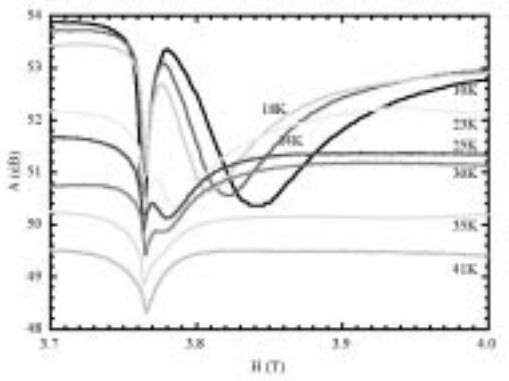

Figure 1. Two absorption ESR peaks merge with increasing temperature.

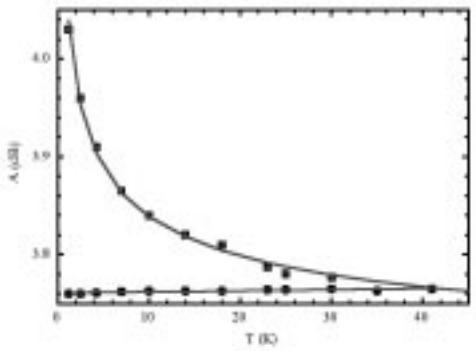

Figure 2. Absorption position H_A vs. temperature (T).

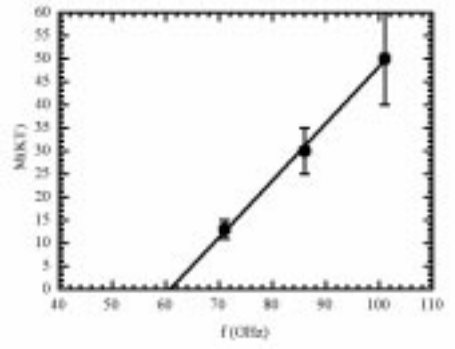

Figure 3. Merging temperature T_M as a function of frequency (f).

at 101 GHz, for a set of temperatures, is shown in Figure 1. It can be seen that two peaks merge at higher temperatures. The H-position of two peaks is shown as a function of temperature in Figure 2. The higher field peak position decreases like $H_A \sim 1/T^{1/3}$.

Measurements at lower frequencies give different merging temperature (Figure 3). Linear fit for these temperatures gives the frequency (field) needed to obtain peak splitting. The splitting offset appears at $f \geq 61$ GHz ($H \geq 2.2$ T).

Reference:

1 Dalal, N.S., *et al.*, J. Chem. Phys., 74, 1916 (1981).

High Magnetic Field Induced Splitting of Electron Paramagnetic Resonance (EPR) Lines in the S=1/2 Heisenberg Antiferromagnet K_3CrO_8

Cage, B., NHMFL/FSU, Chemistry
Brunel, L-C., NHMFL/FSU, Physics
Dalal, N.S., NHMFL/FSU, Chemistry

Recently, multi-frequency electron paramagnetic resonance (EPR) experiments spanning the field range of 0.34 T to 13.3 T were conducted on simple Cr(V), S=1/2, I=0 Heisenberg paramagnets[1] in both the crystalline and powder form. In the compound K_3CrO_8, anomalous splittings of the main EPR line were discovered in both single crystals and powders, which were not easily explained by conventional theory. The magnitude of these splittings was observed to scale with both the applied Zeeman field and temperature. The frequency dependence at 3.7 K is demonstrated in Figure 1. At 110 GHz, there are two pronounced shoulders flanking the main peak. As the frequency is increased to 220 GHz, the main peak is split into a doublet of unequal component intensity. By increasing the frequency to 330 GHz these lines are further split into four peaks, or two pairs of unequal intensity.

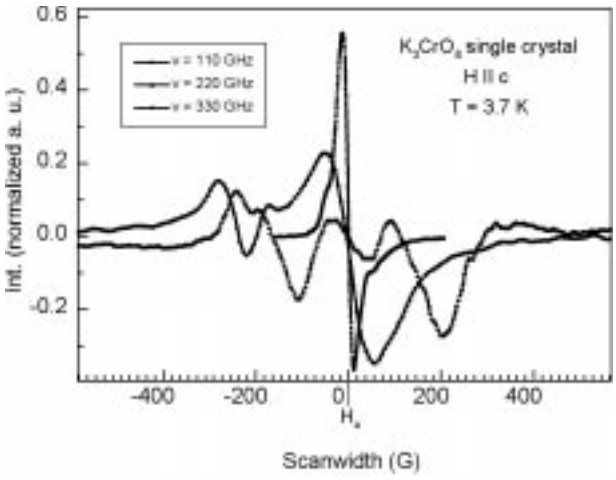

Figure 1. Frequency dependence of a K_3CrO_8 single crystal with H || c at 3.7 K.

Possible Models

(1) Site Splitting

One postulated mechanism is the resolution of inequivalent magnetic sites, or site-splitting. The crystal structure supports such a mechanism because there are two inequivalent chromium atoms per unit cell. The data in Figure 1 are, however, for the H || c crystal orientation, for which such sites should be degenerate, thereby arguing against this mechanism. Furthermore, recent low temperature, high frequency (> 370 GHz) powder data has also demonstrated splitting of the main EPR peaks. Since all symmetry related sites are represented in the powder average, any splittings observed cannot be attributed to site splitting in its normal sense; i.e. chemically equivalent but magnetically inequivalent sites within the crystal structure.

(2) Pair Interaction

A possible explanation for the low temperature splittings is cooperative effects, or pair interaction between neighboring chromium sites at temperatures near the exchange energy (J). Evidence for pair interaction is the observation of antiferromagnetic ordering[2] at ~ 1K.

(3) Field Induced Phase Transition

A temperature dependent magnetic field induced phase transition may be another cause of the anomalous splittings. An indication of this is that at higher fields (> 13 T) some splittings[3] are observable at room temperature. Measurements of the magnetic susceptibility as functions of field and temperature in the ranges of 0 T to 20 T and 1.2 K to 300 K, respectively, are planned to investigate this possibility.

References:

1 Dalal, N.S., *et al.*, J. Chem. Phys., 74, (1981).

2 Singh, K., Doctoral Thesis, (1988).

3 Cage, B., *et al.*, J. Magn. Reson., 135, 178-184, (1998).

Ca-Based Ruthenates: Mott Transitions to Bad Metals

Cao, G., NHMFL
Alexander, C.S., NHMFL
McCall, S., NHMFL
Dobrosavljevic, V., NHMFL
Crow, J.E., NHMFL
Lochner, E., FSU, MARTECH
Guertin, R.P., Tufts Univ., Physics

The Ca-based ruthenate series Ca_2RuO_4, $Ca_3Ru_2O_7$, and $CaRuO_3$ are, respectively, single (Ru-O) layered, double layered, and essentially continuous layered structures. While the first two order antiferromagnetically with decreasing T_N, the latter is paramagnetic, but with a hugely enhanced susceptibility, and only small doping on either the Ca or Ru sites precipitates magnetic order. The series progresses from a highly insulating to a bad metallic ground state, and even at T = 70 K, the electrical resistivity varies by over 14 orders of magnitude between the end members. We have recently discovered a metal insulator Mott transition at T_M=357 K in Ca_2RuO_4, consistent with the previous discovery of T_M = 48 K in $Ca_3Ru_2O_7$ (see Figure 1). Unlike most other such transitions, the Ca_2RuO_4 transition, which goes from a near metallic high temperature paramagnetic phase to a lower temperature highly insulating phase, is not accompanied by magnetic order, but appears to be unique in being driven by a simultaneous high temperature tetragonal to low temperature orthorhombic structural transition. The magnetic susceptibility, $\chi(T)$, shows a small change at T_M, but it then increases rapidly with decreasing temperature with a non-Curie-Weiss (χ_O/T-θ) dependence, and we believe this is related to an incipient structural instability that gives rise to an unstable and variable Ru-O-Ru bond angle. (The value of the magnetic moment and the nature of the Ru-Ru coupling should be a function of the bond angle.)

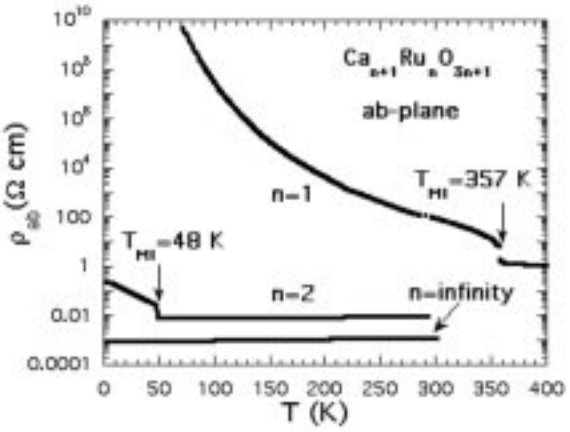

Figure 1. Resistivity ρ(T) in the ab-plane as a function of temperature for n+1,2, and infinity.

The electrical resistivity vs. temperature, ρ(T), in the insulating regimes for both Ca_2RuO_4, and $Ca_3Ru_2O_7$ cannot be fit over any reasonable temperature range with an activation model, ρ(T) = Aexp(Δ/T). However, ρ(T) for Ca_2RuO_4 fits a hopping model including Coulomb interactions (the Efros-Shklovskii model), ρ(T) = Aexp(To/T)$^{1/2}$ over a remarkably large range of resistivity and temperature. This suggests that other non-hopping mechanisms, such as dynamic or static modulation of the Ru-O-Ru bond angle (which is 152°–far from the "ideal" 180°) gives rise to a parabolic curvature of the density of states at the Fermi surface, as this is necessary for $T^{-1/2}$ resistivity. Finally, the low dimensionality and highly "non-ideal" nature of the crystal structure is responsible for the finding that the Ca_2RuO_4 antiferromagnetic insulating properties are totally dissimilar to those of its isomorphic Sr counterpart, which has a superconducting ground state.

Novel Physical Phenomena in Quasi-One-Dimensional $BaIrO_3$

Cao, G., NHMFL
Henning, P., Brookhaven National Laboratory
Lochner, E., FSU, MARTECH
Crow, J.E., NHMFL
Guertin, R.P., Tufts Univ., Physics

$BaIrO_3$ is a monoclinic quasi-one-dimensional compound. The crystal structure consists of trimers of face-sharing IrO_6 octahedra, which are vertex-linked to other trimeric clusters forming columns roughly parallel to the c-axis. Two crystallographically distinct clusters give rise to two different Ir-Ir distances, 2.626 Å and 2.633 Å, which are shorter than the intercluster distances 3.958 Å and 3.975 Å. This allows two types of interactions–direct Ir-Ir bonding for face sharing, and indirect Ir-O-Ir linkages for corner sharing octahedra. It is this unique structure that determines the d-bandwidth, or instability of the Fermi surface, and ultimately unusual physical properties.

As shown in Figure 1a, the system undergoes successive density wave-like transitions along the c-axis at two temperatures, T_{C1} = 26 K, T_{C2} = 173 K, in abrupt features of resistivity, ρ(T). Between these transitions, a sharp peak seen in ρ(T) at T_P = 80 K clearly signals an alteration of electronic states. In contrast, within the ab plane ρ(T) increases as T ⇒ 0 with no precipitous feature, revealing an anisotropy in the conductivity. A magnification of the transitions is seen in the inset of Figure 1a. At T_{C1} = 26 K, there is an abrupt, nearly discontinuous, increase in ρ(T) connecting metallic-like behavior for T_{C1} < T < 80 K with non-metallic behavior for T < T_{C1} (ρ(2 K)/ρ(26 K)≈55), indicative of a significant gapping of the Fermi surface. Below T_{C2}, ρ(T) follows an activation law characteristic of a charge density wave.

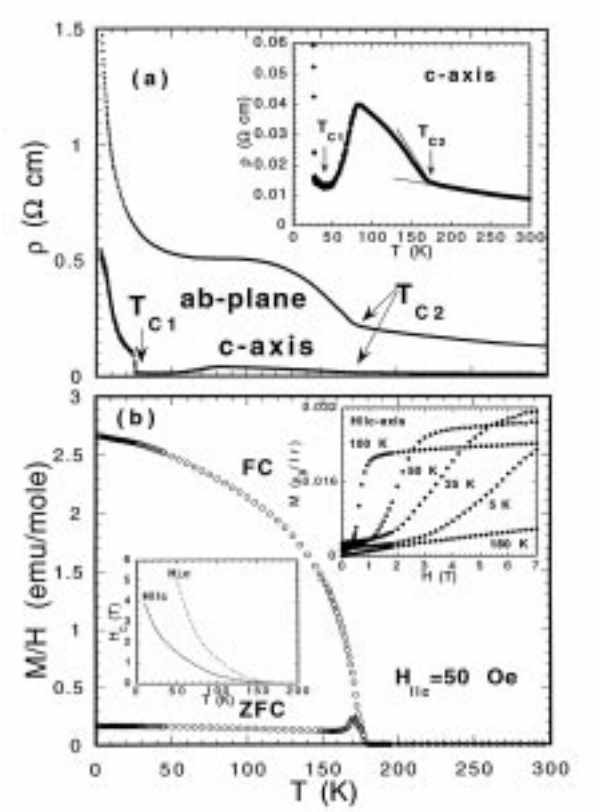

Figure 1. Resistivity ρ and magnetic susceptibility M/H as a function of temperature. Inset in Figure 1(a): An enlarged ρ for the c-axis. Insert in Figure 1(b): Magnetization vs. H for various temperatures. Inset (lower) in Figure (b): Critical field H_c as a function of temperature.

The most unique and significant characteristic is that the transition at T_{C2} is accompanied by a robust ferromagnetic transition (see Figure 1b). Unlike that of ordinary ferromagnets, ρ(T) along with the transition temperature T_{C2}, remains strictly unchanged in magnetic fields up to 10 T, suggesting an anomalous interplay between transport and magnetism that is believed to be associated with the density wave formation.

This contention, the formation of a Peierls distortion-precipitated charge density wave, is further manifested in a variety of experiments:

- X-ray diffraction spectra exhibit satellite peaks below T_{C2} = 173 K, indicating a superlattice structure typical of a CDW;
- Infrared conductivity displays the splitting of phonon lineshapes into three features below T_{C2}, suggesting the presence of a symmetry-breaking process;
- I-V characteristic shows a non-linear conductivity, a prominent feature of a CDW.

Given the fact that the ground state for density waves has so far been found to be either paramagnetic (charge density wave) or antiferromagnetic (spin density wave), a robust density wave with a ferromagnetic ground state, as all experiments conducted indicate, suggests a novelty of this system, and more importantly, a pronounced inconsistency with our understanding of density waves, which were, heretofore, confined to a very restricted group of low dimensional materials.

Weak Ferromagnetism and Anomalous Resistivity in Sr_2IrO_4

Cao, G., NHMFL
Bolivar, J., NHMFL
McCall, S., NHMFL
Crow, J.E., NHMFL
Guertin, R.P., Tufts Univ., Physics

Sr_2IrO_4 orders ferromagnetically at a relatively high temperature, T_c = 240 K, but with an extremely small ordered moment per Ir atom (0.5 μ_B/Ir paramagnetic Curie-Weiss effective moment and 0.14 μ_B/Ir saturation moment). The temperature dependence of the electrical resistivity, ρ(T), and of the low field magnetic moment, M(T), are highly anisotropic, reflecting the low effective dimensionality of the slightly distorted K_2NiF_4 crystal structure, the same structure as the original high T_c cuprate superconductors. These studies were the first made in single crystal samples of Sr_2IrO_4.

Several surprising features were found in the transport measurements: First, ρ(T), generally increases weakly with decreasing temperature, but unlike all the other ruthenate and iridate compounds studied to date, shows no anomaly at the well-defined magnetic transition at T_c = 240 K. Second, ρ(T) measured along the a-axis (easy axis for magnetization), suddenly begins to decrease again at about T = 20 K, and continues to decrease down to at least T = 0.1 K (unpublished data), an effect that is not at all understood. Third, ρ(T) cannot be fit over any reasonable temperature range to an activation resistivity, $\rho(T) = A\exp(\Delta/T)$, but does obey three dimensional variable range hopping for 190 < T < 300 K. Finally, the current dependence of the resistivity, i.e., ρ(J) at fixed T < T_c shows highly non-linear (non-Ohmic) behavior, notably negative differential resistivity, dI/dV < 0, both along the a- and c-axes. This behavior is seen in related ruthenates and iridates, which are close to a metal-insulator transition.

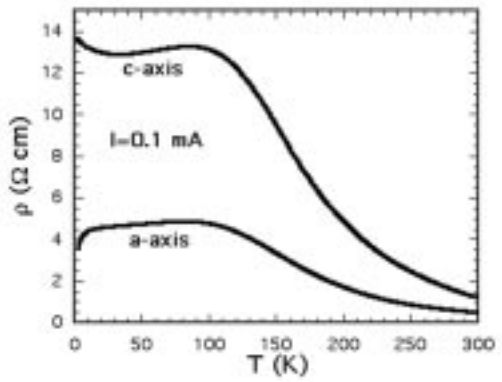

Figure 1. Resistivity ρ(T) vs. temperature for the a- and c-axis.

The magnetic properties are equally anisotropic; the easy axis for magnetization is found to be along the a-axis. The magnetic susceptibility for T > T_c is Curie-Weiss-like; and the isothermal magnetization shows a spin-flop like transition at about 0.2 T at low temperatures. The saturation magnetic moment, however, is far less than the value expected for the low spin Ir^{4+} (d^5) configuration, namely $1m_B$/Ir, probably due to weak band splitting in this nearly metallic itinerant system. The anomalous properties of Sr_2IrO_4 are attributed to a highly distorted non-ideal structure (the Ir-O-Ir bond angle is 157°–far from the ideal 180° value), extended 5d orbitals compared to their 3d counterparts–orbitals that couple strongly to the p orbitals of nearby O atoms, and the proximity of Sr_2IrO_4 to the metal-nonmetal interface.

Correlation Between Spin Polarization and Magnetic Moment in Ferromagnetic Alloys

Choy, T.S., UF, Physics
Chen, J., UF, Physics
Hershfield, S., UF, Physics/NHMFL

Since the 1970's ferromagnet-insulator-superconductor tunneling experiments have shown that the electron spin polarization in the density of states at the Fermi energy for Fe, Co, and Ni is positive.[1] Assuming that the tunneling conductance is proportional to the total density of states at the Fermi level, a straight forward application of the Stoner-Wohlfarth-Slater theory of ferromagnetism predicts negative spin polarizations for Co and Ni. Furthermore, the actual size predicted spin polarization seen experimentally differs by up to an order of magnitude.

One correlation which is found experimentally is that the tunneling density of states seems to track the magnetization. As one varies the composition in a wide range of Ni alloys, one finds that the polarization in the tunneling density of states increases with the magnetization. This is quite surprising because the band structure of the transition metals is complicated, and it is not clear why the electron spin polarization at the Fermi surface should be related to the magnetization, which is a property of the entire Fermi sea.

To understand this correlation, we have performed a self-consistent tight-binding coherent potential approximation calculation for a number of ferromagnetic alloys. We compute both the net

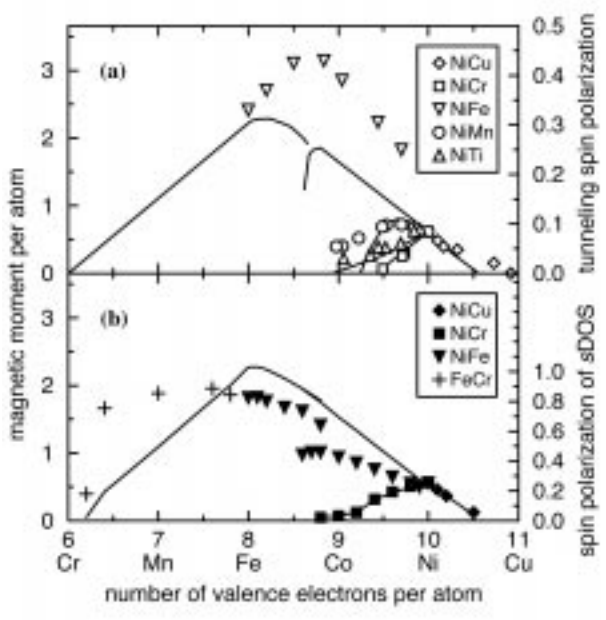

Figure 1. Comparison of the magnetic moment per atom (solid curves) and spin polarization at the Fermi energy (symbols) for (a) experiment and (b) theory.

magnetization and the spin polarization of the s-density of states at the Fermi energy. As illustrated in Figure 1(b), the results of our calculation for both the magnetic moment per atom (solid curves) and the spin polarization of the s-density of states at the Fermi energy (symbols) follow the same trends that the spin polarization of the measured density of states and magnetic moment per atom shown in Figure 1(a). This resolves the above puzzles and provides strong evidence that the tunneling measurements are dominated by the s-electrons, which is in agreement with other recent experimental and theoretical work.

Reference:

1 Meservey, R., *et al*., Phys. Rep., 238, 173 (1994).

Magnetization and de Haas-van Alphen Measurements to 50 T on $CeRhIn_5$

Cornelius, A.L., LANL
Arko, A.J., LANL
Sarrao, J.L., LANL

We have performed magnetization and de Haas-van Alphen (dHvA) measurements in pulsed fields to 50 T on the antiferromagnet $CeRhIn_5$. The measurements were performed with the magnetic field applied along the (100) and (001) axes of the tetragonal crystal. There is a magnetic transition at B=2 T and T=0.5 K when B||(001). When the signal is plotted versus the inverse field, one observes oscillations in the signal with a frequency that is directly proportional to an extremal area of the Fermi surface; this is the dHvA effect. Plots of the fast Fourier transform (FFT) of the signal versus inverse field are shown in Figure 1 for B||(100) in (a) and B||(001) in (b). From Figure 1, numerous dHvA frequencies can be observed with effective

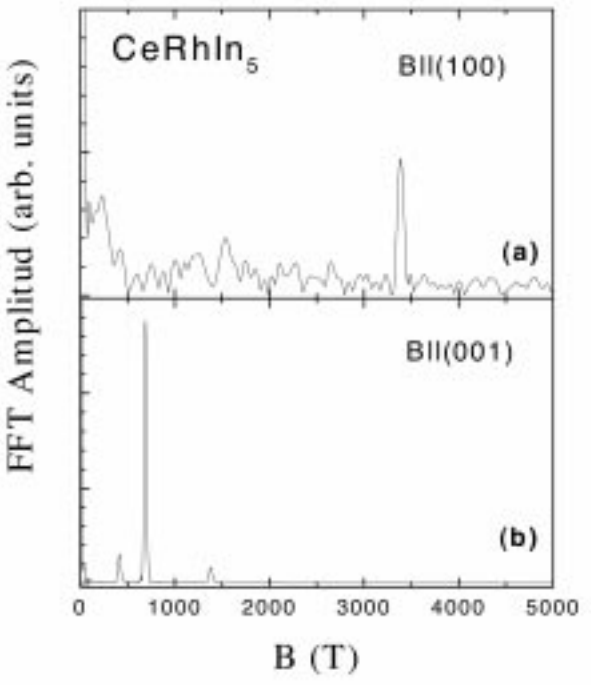

Figure 1. The fast Fourier transforms (FFT) of the de Haas-van Alphen signal measured at T=0.5 K for $CeRhIn_5$ for B||(100) in (a) and B||(001) in (b).

masses ranging from 0.5 m_e to 3 m_e. Also, due to the differences in the dHvA results for the different field directions, there is a great deal of anisotropy to the Fermi surface. We are undertaking a complete determination of the Fermi surface by the use of angle-resolved dHvA measurements.

Coercivity in $SmCo_5$ Magnets

de Campos, M.F., USP-Brazil, Engineering
Saito, N.H., IPT-Brazil
Landgraf, F.J.G., IPT-Brazil
Romero, S.A., USP-Brazil, Physics
Neiva, A.C., USP-Brazil, Engineering
Missell, F.P., USP-Brazil, Physics

A series of six alloys was produced[1] with compositions ranging from 16.43 to 17.38 at.% Sm. Two series of magnets were produced from these alloys, one (S) of which was only sintered at 1150 °C, while the other (ST) was both sintered and treated at 850 °C. For the magnets of series S, the coercive field, H_c, is considerably smaller than for those of series ST. It was not possible to attribute the coercivity differences observed in the two series of magnets to microstructural differences and precise lattice parameter, and Curie temperature measurements were also unable to reveal any difference between the two series of magnets. The last intrinsic property that must be investigated to see if it can explain the differences in coercivity is the anisotropy field H_A. Preliminary measurements made at the NHMFL using static magnetic fields of 33 T allowed us to draw two main conclusions:

(1) Our measurements indicate that the anisotropy field $\mu_o H_A$ of $SmCo_5$ is larger than values cited in the literature. Experimental curves for several samples were extrapolated to estimate $\mu_o H_A$ = 50-55 T.

(2) Using data obtained between 10 T and 32 T, we determined the anisotropy constants K_1 and K_2, as well as the anisotropy field $H_A = (2K_1 + 4K_2)/2M_s$ for some magnets. The average values obtained for seven magnets are $K_1 = 14 \times 10^6$ J/m^3, $K_2 = 5 \times 10^6$ J/m^3, and $\mu_o H_A$ = 53 T.[1]

On the other hand, it was not possible to verify a possible correlation between the anisotropy fields of the S and ST magnets and their respective coercive fields. This was the case because we did not obtain reliable measurements of magnetization curves for S and ST magnets of the same composition. Further measurements were performed using a new hardened Be-Cu sample holder and a reinforced drive rod, as well as additional spacers on the magnetometer drive rod. Although these improvements helped to maintain the relative orientation of the samples and the magnetic field, and provided more reliable data, an unacceptably high noise level was observed on curves for the perpendicular orientation. This problem will be resolved by reducing the sample size for future measurements.

References:

1 de Campos, M.F., *et al.*, J. Appl. Phys., 84, 368-373 (1998).

Antiferromagnetic Resonance as a Tool for Investigating Magnetostructural Correlations: The Canted Antiferromagnetic State of $KMnPO_4 \cdot H_2O$ and a Series of Manganese Phosphonates

NHMFL

Fanucci, G.E., UF, Chemistry
Krzystek, J., NHMFL
Meisel, M.W., NHMFL/UF Physics and Center for Ultralow Temperature Research
Brunel, L.-C. NHMFL
Talham, D.R., NHMFL/UF, Chemistry

Antiferromagnetic resonance (AFMR) has been used to characterize the canted antiferromagnetic state and to probe magnetostructural correlations of a series of layered solids including $KMnPO_4 \cdot H_2O$, four manganese alkylphosphonates, $Mn(O_3PC_nH_{2n+1}) \cdot H_2O$ n = 3 - 6, and

manganese phenylphosphonate.[1] All samples were investigated as powders. The high field EMR facilities at NHMFL, with field sweep capabilities from 0 T to 17 T, the availability of several frequency sources, and variable temperature capabilities, make this technique applicable to a wide range of materials. Since the superexchange pathways in these materials are nearly identical, the observed differences in the magnetic exchange are thought to arise from electronic perturbations caused by the phosphate/phosphonate substituents. It was observed that the symmetric exchange field decreased as the electron donating ability of the substituent decreased. Analysis of the frequency and field dependence of the AFMR signals revealed that the canting angle, β, for these materials was 0.7-0.9° ± 0.2°. In addition, the anisotropy of the magnetic interactions was determined from analysis of the frequency and field dependence of the AFMR signals. Some of the advantages of AFMR over other microscopic probes have been demonstrated, including high sensitivity to subtle differences in magnetic interactions, and the ability to work with a small amount of material.

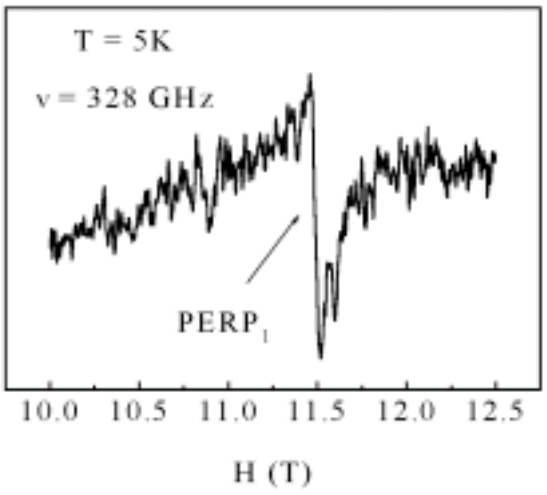

Figure 1. AFMR signal from a 100 layer MnODP LB film oriented with the magnetic easy-axis perpendicular to the applied magnetic field.

The method has now been extended to Langmuir-Blodgett (LB) films, the first measurement of its kind on thin film samples (see Figure 1). Antiferromagnetic resonance signals have been observed for an LB film of manganese octadecylphosphonate (MnODP). The MnODP film sample for AFMR measurements consisted of 100 layers and spectra were obtained in transition mode. The splitting of the PERP2 signal is attributed to different orientations of the sample pieces.

Reference:

1 Fanucci, G.E., *et al*., J. Am. Chem. Soc., 120, 5469-5479 (1998).

Hall Effect and Thermopower of $RESb_2$ Compounds

Gamble, B.K, Clemson Univ., Physics
Kuo, Y.K., Clemson Univ., Physics
Tessema, G.X., Clemson Univ., Physics
Canfield, P., Ames National Laboratory and Iowa State Univ., Physics
Lacerda, A.H., NHMFL/LANL

We have investigated the temperature (T) dependence of the Hall coefficient of several compounds of the $RESb_2$ family of compounds; RE stands for Pr, La, Nd, and $AgLaSb_2$, etc. These are layered compounds synthesized by P. Canfield. The compounds attracted recent interest due to their low dimensionality and metamagnetic and antiferromagnetic transitions observed at low T. Particular attention was given to $PrSb_2$, which exhibits a resistance anomaly at 100 K. This anomaly is attributed to the possibility of a charge density wave transition.

With Mike Hundley (MST-10 Los Alamos), we conducted a detailed study of the thermoelectric power, which confirmed that a dramatic change in density of states takes place at 100 K in this compound. The ac-specific heat exhibits a cusp at 100 K, and confirms that the resistance anomaly at 100 K is due to a phase transition. Using the 20 T dc magnet at NHMFL-Los Alamos, we conducted a systematic study of the T dependence of the Hall voltage. Figure 1 shows that the Hall resistance increases rapidly between 100 K and 5 K. An

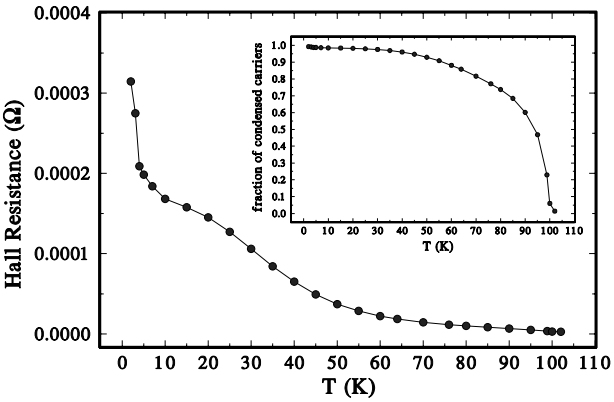

Figure 1. The temperature (T) dependence of the magnitude of the -R_H, Hall resistance. The inset shows the T dependence of the estimated fraction of condensed electrons.

additional steep rise is also seen below 5 K. Assuming that this increase in the Hall constant is due to a DW driven carrier concentration, we estimate that nearly 90% of the carriers are condensed at 5 K. This is shown in the inset, the T dependence of the condensed carriers is nearly BCS-like. Hall measurements in the other compounds have been complicated by large extraordinary components.

This work was supported by a grant from NHMFL and the NSF, Grant Number DMR9312530.

The Fermi Surface of Ferromagnetic EuB_6

Goodrich, R.G., Louisiana State Univ., Physics
Teklu, A., Louisiana State Univ., Physics
Harrison, N., NHMFL/LANL
Vuillemin, J.J., Univ. of Arizona, Physics
Hall, D., NHMFL
Young, D., NHMFL
Fisk, Z., NHMFL
Sarrao, J., LANL

We have determined the Fermi surface and effective masses of electronic carriers in ferromagnetic EuB_6 from pulsed field magnetization and steady field torque Landau quantum oscillatory measurements. To aid in the interpretation of the measurements, SQUID magnetometer measurements of the overall magnetization were made on the same samples. The results are consistent with recent electronic structure calculations and show that both an electron and a hole pocket are located at the X point in the Brillouin zone.

High field dHvA magnetization measurements to 60 T with the field directed along the <100> axis of the cubic structure were made using the NHMFL Pulsed Field Facility at the Los Alamos National Laboratory. Intermediate field, to 24 T, oscillatory torque measurements were made using a cantilever magnetometer in a resistive magnet at Tallahassee. For the torque measurements, *in situ* rotations of the sample with respect to the applied field were made with the field applied in a (100) plane.

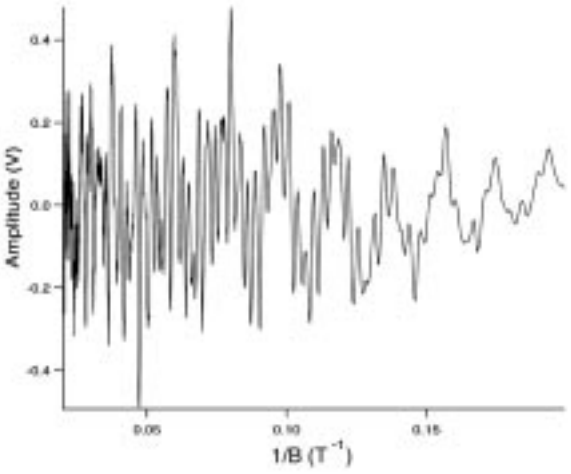

Figure 1. dHvA signal amplitude in EuB_6 as a function of the reciprocal of the applied magnetic field.

.

An example of the oscillatory magnetization data from a down sweep of the pulsed field plotted vs. 1/B is shown in Figure 1. There are four frequencies present in this data corresponding to the maximum and minimum areas of two ellipsoidal shaped pockets of carriers. We have assigned the smaller pocket to holes and the larger to electrons to give the best agreement with previously published Hall effect,[1] plasma frequency[2] data, and energy band calculations.[3] From the lack of observation of spin splitting in

the lowest frequency data and the harmonic amplitudes of this frequency, we also conclude that the hole band is spin split with one spin state above and one below the Fermi energy.

References:

1 Guy, C.N., *et al*., Solid State Commun., 33, 1055 (1980).
2 Degiorgi, L., *et al*., Phys. Rev. Lett., 79, 5134 (1997).
3 Massidda, S., *et al*., Phys. B, 102, 83 (1997).

Lattice and Magnetic Effects in Doped Manganites

Gor'kov, L.P., NHMFL
Kresin, V.Z., Lawrence Berkeley Laboratory

The recent activity relating to manganites is stimulated by the potential of the "colossal" magnetoresistance (CMR). Although the consensus exists that the main players in the phenomenon are the double exchange (DE) mechanism together with the Jahn-Teller(JT) degeneracy on the Mn^{3+}-sites, there are problems with understanding important physical details. The central issue that brings manganites closer to cuprates, is the mechanism of doping. In other words, it is not understood yet how adding divalent atoms, $La_{1-x}A_xMnO_3$, develops a conducting network.

From this and other points of view, it is again important to understand whether electron-electron correlations, leading to localization of the electrons states are the necessary ingredient for understanding manganites properties. The stoichiometric $LaMnO_3$ is an insulator and the A-phase antiferromagnet. The usual interpretation of such a structure is based on the picture of the indirect anisotropic exchange of the spins on the Mn-sites. The first step done in Reference 1 was to show that such a structure can equally be described in terms of a band insulator.

As far as doping is concerned, the most nontrivial feature in the concentration dependence seems to be the existence of the concentration threshold, $x_c \simeq 0.16$, above which the metallic conductivity (at low T) sets in. In addition to the different scenarios, such as a phase transition (or a quantum phase transition) at this specific concentration, we suggested an explanation of the phase diagram of manganites (at $x<0.5$) based on the percolative approach. Namely, it assumes that the doped holes (Mn^{4+}) are localized close to divalent dopants. With the concentration increase a percolative path is formed that is also a "spine" for the conducting cluster at higher concentrations. This view suggests the existence of "islands" of other phase which would result in strongly inhomogeneous (spatially and on the time scale) structure of doped manganites. This conclusion is supported by numerous experiments: magnetic neutron scattering, the so-called "pair distribution" analysis, NMR-data, elastic neutron scattering indicating in favor of some droplets inclusions.

In addition to that, in References 2 and 3, it is also shown that the percolative approach may be extended to the mechanism of CMR itself: with the field increase, concentration of the ferromagnetic (and conducting) phase also increases shifting the percolative threshold up, to somewhat higher temperatures. The immediate way to verify the applicability of these ideas is the use of the Kirkpatrick relation, i.e., proportionality in the temperature dependence of conductivity near T_c and the so-called "stiffness" coefficient which determines the low energy spin-wave spectrum and magnetization. All three quantities were measured on the same samples by the NIST-Maryland group. The critical behavior of all characteristics follows well this relation.

References:

1 Gor'kov, L.P., *et al*., JETP Lett., 67, 985 (1998).
2 Gor'kov, L.P., Physics-Uspekhi, 41, 589 (1998).
3 Gor'kov, L.P., *et al*., J. Supercond., 12, 243 (1999).

Faraday Rotation in Paramagnetic Salts Under High Magnetic Field

Guillot, M., CNRS/MPI

Although there exists, in the literature, a large number of experimental studies devoted to the magneto-optical (MO) effects in magnetic ceramics, the applied magnetic field is usually limited to low values. Furthermore, the theoretical analysis of the MO properties are very scarce and different questions such as the relationship between the magnetization and the MO effects, the role of the spin-orbit interaction strengths of the fundamental and (or) excited electronic configurations, the influence on the MO properties of the symmetry of the magnetic site (crystal field effect) remain unsolved. References 1 and 2 offer an illustration of the complexity of the problem, the Faraday rotation that represents the first-order (in magnetization) MO effect being governed by four parameters: temperature, magnetic field (i.e. exchange and (or) external applied field), wavelength of the incident linearly polarized light, and orientation of the magnetization vector.

To avoid the hazardous separation of the sample and window-cryostat contributions, the polarizer and the analyzer are located in the very vicinity of the sample in the low temperature chamber at the center of the high field magnet. Very thin (200 microns) optical fibers are used to conduct the light from the source to the polarizer and from the analyzer to the detector. When the analyzer behind the sample is eliminated, the absorption spectra of the sample can be directly obtained.

Most experiments were performed in the visible range at three different wavelengths (633, 450 and 550 nm). Figure 1, where the isothermal high field variations of the Erbium Gallium Garnet (ErGaG) are reported, illustrates the quality of measurements. A part of the so-obtained results for ErGaG and for the trifluoride of neodymium NdF_3 was already published.[3,4] Magnetization (M) has been measured in the same single crystals. At low temperature, Fr and M are proportional only when the magnetization is weak but in medium and high magnetic field, complex relationships between M and FR are found.

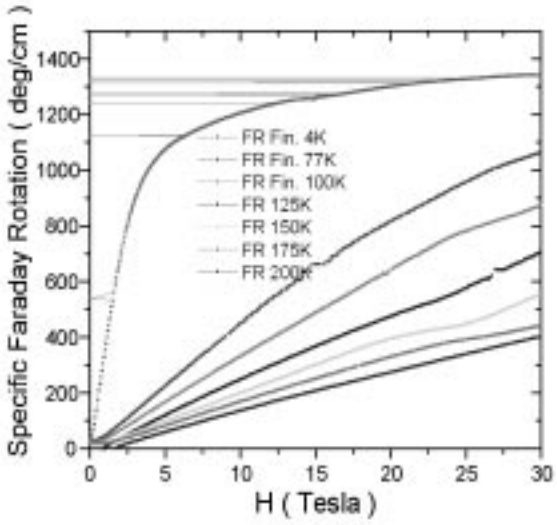

Figure 1. Isothermal variations of the Faraday rotation under high magnetic field at 633 nm wavelength in the Erbium Gallium Garnet; external field applied along the [111] direction.

References:

1 Yang, J., *et al*., Phys. Rev. B, 56, 17, 11119-11133 (1997).

2 Yang, J., *et al*., oral presentation at 43rd Annual Conference on Magnetism Magnetic Materials, Miami, FL, November 9-12, 1998; to be published in J. Appl. Phys.

3 Guillot, M., *et al*., J. Appl. Phys., 83 (11) 6762 (1998).

4 Guillot, M., *et al*., oral presentation at 43rd Annual Conference on Magnetism Magnetic Materials, Miami, FL, November 9-12, 1998; to be published in J. Appl. Phys.

Effect of Spin-1 Impurities in Dimerized Heisenberg Chains

Hansen, P., Instituto de Fisica Rosario, Rosario, Argentina
Riera, J., Instituto de Fisica Rosario, Rosario, Argentina
Delia, A., NHMFL
Dagotto, E., NHMFL/FSU, Physics and MARTECH

The effects of spin-1 impurities introduced in dimerized antiferromagnetic spin chains are studied using Lanczos diagonalization and quantum Monte Carlo simulations.[1] Firstly, the magnitude of the interaction between a Ni-ion replacing a Cu-ion is derived for the case study system Cu-O-Cu. Then, it is shown that the introduction of S = 1 impurities leads to the suppression of the original spin gap of the dimerized system, and to the enhancement of the antiferromagnetic correlations close to the impurity. These features are interpreted in terms of a valence bond picture of the ground state of both the pure and the doped system. The similitudes and differences between the underlying mechanisms that produce these effects in the cases of nonmagnetic and S = 1 impurities are analyzed. It is stressed that a singlet formed between the spin-1 impurity site, and the two spin-1/2 neighbors spins behaves as an effective nonmagnetic vacancy that may be partially responsible for the enhancement of the antiferromagnetic correlations on the whole system. Implications of these results for experiment are also discussed.

Reference:

1 Hansen, P., *et al*., Phys. Rev. B, 58, 6258 (1998).

Effects of Exchange Interaction Between Mn^{++} and Conduction Electrons on Mn^{++} EPR

Hassan, A.K., NHMFL
Saylor, C.A., NHMFL
Brunel, L.-C., NHMFL
Yang, G., Univ. of Notre Dame, Physics
Furdyna, J.K., Univ. of Notre Dame, Physics

Studies of diluted magnetic semiconductors (DMS) have shown that, when a part of the semiconductor lattice is replaced by substitutional magnetic ions, the exchange interaction between these ions and band electrons leads to enormous Zeeman splittings of electronic levels when an external magnetic field is applied.[1] The reverse effect—the modification of atomic levels of Mn^{++} induced by exchange interaction with spin-polarized electrons surrounding the Mn^{++} ion—can also take place. Our analysis indicates that this effect will manifest itself through the shift of electron paramagnetic resonance (EPR) of Mn^{++}, which in turn provides an experimental handle on the value of the Pauli susceptibility of the electron gas.[2]

In order to explore exchange-induced effects of free carriers on EPR of magnetic ions, EPR measurements were made on powder samples of the narrow-gap semiconductor $Hg_{1-x}Mn_xSe$ containing dilute concentrations of Mn (x = 0.001, 0.03, and 0.05) at high magnetic fields, at a series of mm frequencies and temperatures. Typical values of the carrier concentration (n) are expected to lie in the range of 5×10^{18} down to 2×10^{17}. The spectra showed significant EPR line shifts as a function of temperature, Mn concentration, and magnetic field. Figure 1 shows the EPR spectra at 187 GHz for x = 0.05 and at different temperatures, where it can be noted that the resonance field of the Mn^{++} EPR line is shifting towards lower fields as the temperature is decreased. In order to bring out the magnitude of the effect of conduction electrons on Mn^{++} EPR, we compare these results with EPR spectra observed on $Cd_{1-x}Mn_xSe$ for similar

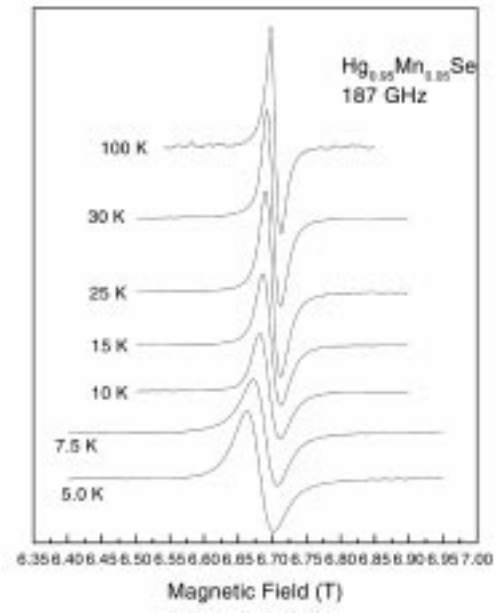

Figure 1. Resonance field shift as a function of temperature in $Hg_{0.95}Mn_{0.05}Se$.

concentrations of Mn, in which the effects of free carriers are expected to be negligible. The shift in resonance field between two temperatures, e.g. 100 K and 5 K, is of the order of 80 G in $Cd_{0.95}Mn_{0.05}Se$ and 220 G in $Hg_{0.95}Mn_{0.05}Se$, measured at the same frequency (220 GHz). This additional shift in the $Hg_{1-x}Mn_xSe$ compounds, as well as the line shifts observed as a function of field, Mn concentration and temperature, are tentatively attributed to changes in the g-factor of the Mn^{++} ions due to the spin polarization of band electrons and the effects of the exchange interaction between the Mn ions and the conduction electrons, as theoretically predicted by Yang, *et al.*[2]

References:

1 Furdyna, J.K., J. Appl. Phys., 64, R29 (1988).

2 Yang, G., Ph.D. Thesis, Univ. of Notre Dame, 1993 (unpublished); Yang, G., *et al.*, Phys. Rev. B (in press).

Magnetic Field Dependence of the Optical Conductivity in a-$Si_{1-x}RE_x$ Alloys

Henning, P.F., Univ. of California, San Diego (UCSD), Physics, and Brookhaven National Laboratory

Basov, D.N., UCSD, Physics

Zink, B., UCSD, Physics

Hellman, F., UCSD, Physics

Dynes, R.C., UCSD, Physics

We have studied the magnetic field (0 T to 15 T) dependence of the conductivity (30cm^{-1} to 4000 cm^{-1}) in a-$Si_{1-x}RE_x$ (RE = Y, Gd) thin films in the vicinity of the metal-insulator transition. The conductivity was calculated from the measured transmission using a novel Kramers-Kronig technique we have developed, which allows for a separation of the Si substrate effects from the effects of the film at all frequencies. For non-magnetic Y doping, there is no measurable magnetic field dependence to the conductivity. In contrast, Gd-doped films reveal large field-induced enhancement of the optical conductivity starting from $\omega = 0$ and extending up to 4000 cm^{-1}. Data for a-$Si_{.85}Gd_{.15}$ at 5 K is shown in the figure.

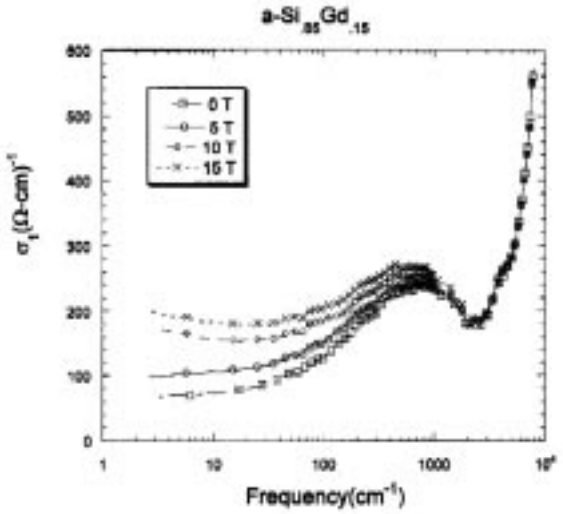

Figure 1. Calculated real part of the conductivity vs. frequency for a-$Si_{.85}Gd_{.15}$ at 5 K for fields of 0, 5, 10, and 15 T.

Sum-rule analysis shows that the effective spectral weight associated with the response of free carriers is strongly temperature and field dependent. We also are investigating the possible effects of photo-induced conductivity on the measurement.

This work was performed at the NHMFL in Tallahassee.

High Field Studies of the Magnetism of Two Dimensional Heisenberg Antiferromagnets

Landee, C.P., Clark Univ., Physics
Turnbull, M.M., Clark Univ., Physics

Low dimensional S=1/2 Heisenberg antiferromagnets are among the simplest many body systems in which quantum fluctuations play a dominant role, and for which quantitative theoretical predictions can be made. We are developing new families of S=1/2 low dimensional Heisenberg antiferromagnets (1D and 2D HAFs) with small exchange strengths so the field dependence of their physical properties can be studied. We have created a new family of 2D HAFs in which S=1/2 copper (II) ions are linked together into magnetically interacting layers by pyrazine molecules with exchange constants in the range 15 K to 25 K that correspond to saturation fields of less than 60 T. Isolation between layers is determined by the spacing provided by the bridging nitrate ions in $[Cu(pz)_2(NO_3)](PF_6)$, and by the bulk of the perchlorate ions for $Cu(pz)_2(ClO_4)_2$.

The magnetization curves for the two compounds were measured at 1.5 K in pulsed fields up to 60 T. The reduced low temperature magnetization curves (M/M_{sat}) of the two compounds are shown in Figure 1, along with the curves for two other 2D HAFs with weaker exchange strengths based on $CuBr_4^{2-}$ layers.[1] The saturation fields for $[Cu(pz)_2(NO_3)](PF_6)$ and $Cu(pz)_2(ClO_4)_2$ are

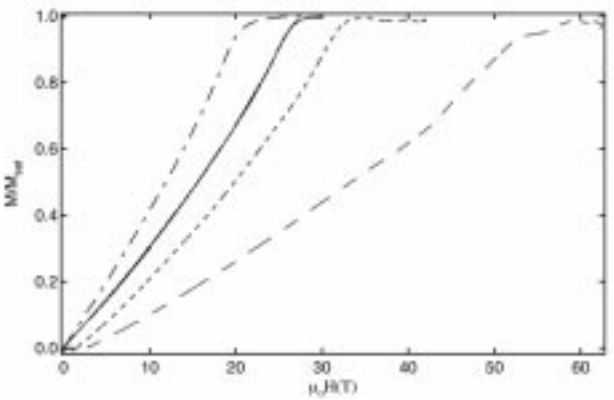

Figure 1. Low temperature reduced magnetizations (M/M_{sat}) as a function of applied field ($\mu_0 H$) for (2-NH_2-5-mepy)$CuBr_4$ (dot dash), (2-NH_2-5-Clpy)$CuBr_4$ (solid line), $[Cu(pz)_2(NO_3)](PF_6)$ (short dashes), and $Cu(pz)_2(ClO_4)_2$ (long dashes).

estimated to be 32.5 T and 53 T, respectively. Every experimental curve shows a characteristic upward curvature, which has recently been explained as being due to a suppression of the quantum fluctuations.[2]

When plotted as (M/M_{sat} versus H/H_{sat}), all four curves in Figure 1 collapse onto a universal curve (not shown), despite the different amount of 3D interactions within the compounds. This universal curve is very well described by the theoretical[2] and numerical[3] predictions for the 2D HAF with no adjustable parameters.

References:

1 Albrecht, A.S., *et al.*, Mol. Cryst. Liq. Cryst., 305, 333 (1997).
2 Zhitomirshy, M.E., *et al.*, Phys. Rev. B, 57, 5013, (1998).
3 Troyer, M., private communication.

Enhancement of Antiferromagnetic Correlations Induced by Nonmagnetic Impurities: Origin and Predictions for NMR Experiments

NHMFL

Laukamp, M., NHMFL
Martins, G., NHMFL
Gazza, C., NHMFL
Malvezzi, A., NHMFL
Dagotto, E., NHMFL/FSU, Physics and MARTECH
Hansen, P., Instituto de Fisica Rosario, Rosario, Argentina
Lopez, A., Instituto de Fisica Rosario, Rosario, Argentina
Riera, J., Instituto de Fisica Rosario, Rosario, Argentina

Spin models that have been proposed to describe dimerized chains, ladders, two dimensional antiferromagnets, and other compounds, are studied here when some spins are replaced by spinless vacancies, such as it occurs by Zn doping.[1] A small percentage of vacancies rapidly destroys the spin gap, and their presence induces enhanced antiferromagnetic correlations near those vacancies. The study is performed with computational techniques, which includes Lanczos, world-line Monte Carlo, and the Density Matrix Renormalization Group methods. Since the phenomenon of enhanced antiferromagnetism is found to occur in several models and cluster geometries, a common simple explanation for its presence may exist. It is argued that the resonating-valence-bond character of the spin correlations at short distances of a large variety of models is responsible for the presence of robust staggered spin correlations near vacancies and lattice edges. The phenomenon takes place regardless of the long distance properties of the ground state, and is caused by a "pruning" of the available spin singlets in the vicinity of the vacancies. The effect produces a broadening of the low temperature NMR signal for the compounds analyzed here. This broadening should be experimentally observable in the structurally dimerized chain systems $Cu(NO_3)_2 \cdot 2.5H_2O$, $CuWO_4$, $(VO)_2P_2O_7$, and $Sr_{14}Cu_{24}O_{41}$, in ladder materials such as $SrCu_2O_3$, in the spin-Peierls systems $CuGeO_3$ and NaV_2O_5, and in several others since it is a universal effect common to a wide variety of models and compounds. In addition, it is argued that the Néel order observed in $SrCu_2O_3$ upon Zn doping is induced by the local antiferromagnetic order discussed in this paper, enhanced by a favorable ratio between the actual Heisenberg couplings along chains and rungs, as reported in recent experimental literature. Based on this reasoning it is here predicted that other ladder materials such as Zn-doped $Cu_2(C_5H_{12}N_2)_2Cl_4$ will not present Néel order at small Zn concentrations.

Reference:

1 Laukamp, M., *et al*., Phys. Rev. B, 57, 10755 (1998).

MEMS Magnetometry in Pulsed Magnetic Fields

Leone, M.J., SUNY Buffalo, Physics
Oh, J.I., Boston College, Physics
Naughton, M.J., Boston College, Physics

We have previously demonstrated the use of cantilever magnetometry in pulsed magnetic fields, for magnets of pulse length ~100ms.[1] Experiments conducted at LANL have now extended the regime of applicability of cantilever magnetometry to that of short pulse magnets (pulse length ~10 ms).[2] Our devices are silicon MEMS sensors in the form of cantilevers or rectangular membranes with resonant frequencies from 1500 Hz to 5000 Hz, as compared to the dc-field cantilever device, whose eigenfrequency is around 1 kHz. Such higher frequencies are preferred in the short pulse environment in order to minimize acoustic interference.

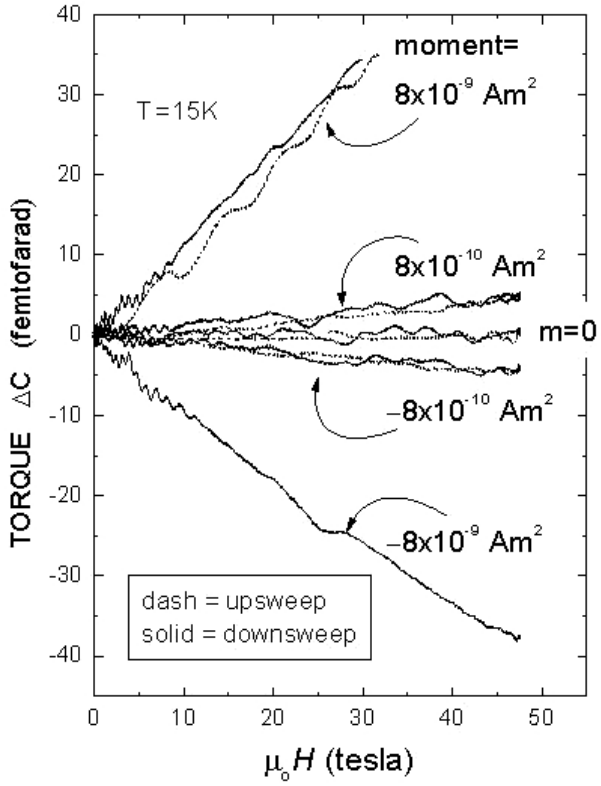

Figure 1. Response of one cantilever to applied moments of 0, 8x10^{-10} Am^2, and 8x10^{-9} Am^2 (10^{-10} Am^2 = 10^{-7} emu).

Some units contain integrated calibration loops, which we have employed to test the response in the LANL short pulse magnets. The application of a constant current provides a constant magnetic moment. The cantilever was mounted such that the calibration loop was perpendiculiar to the applied magnetic field (maximum torque). The accompanying figure shows the response of one cantilever to applied moments of 0, 8x10^{-10} Am^2, and 8x10^{-9} Am^2 (10^{-10} Am^2 = 10^{-7} emu). As can be seen, the device responds linearly with applied field, as expected. The equivalent noise bandwith for this particular device is measured to be δm_{RMS}=4x10^{-13} Am^2/Hz$^{1/2}$, demonstrating that MEMS magnetometry can be used in pulsed magnetic fields to better than 10^{-7} emu.

References:

1 Naughton, M.J., *et al.*, Rev. Scient. Instrum., 68, 4061 (1997); Naughton, M.J., *et al.*, Physica B 246-247, 125 (1998).

2 Leone, M.J., *et al*., Bull. Am. Phys. Soc., 43, 463 (1998).

High Field EPR of the Strongly Coupled $Cd_{(1-x)}Mn_{(x)}Se$ and $Cd_{(1-x)}Mn_{(x)}S$ Magnetic Semiconductor Alloys

McCarty, A.D., NHMFL/FSU, Physics
Hassan, A.K., NHMFL
Martins, G.B., NHMFL
Furdyna, J.K., Univ. of Notre Dame, Physics
Brunel, L.-C., NHMFL

High field EPR proves to be a powerful tool for probing the magnetic interactions of magnetic semiconductors, and we have applied this technique to the investigation of two semiconductor alloy systems: $Cd_{1-x}Mn_xSe$ and $Cd_{1-x}Mn_xS$. The Mn^{2+} ions in these alloys are strongly coupled, and the nature of the Mn^{2+}-Mn^{2+} interactions is revealed in the linewidth and resonance position of the EPR spectrum. In the EPR spectra of these alloys, the linewidth broadens as the temperature decreases, as Mn^{2+} concentration increases, and as the anion size increases. The Dzyaloshinski-Moriya (DM) interaction, which is an anisotropic superexchange process,[1] is the possible explanation for the broadening with increasing anion size, because its strength increases with increasing anion size. This assumption is supported by the theoretical work of Larson, *et al*., who showed that the main contribution to the Mn^{2+}-Mn^{2+} exchange interaction is from superexchange.[2]

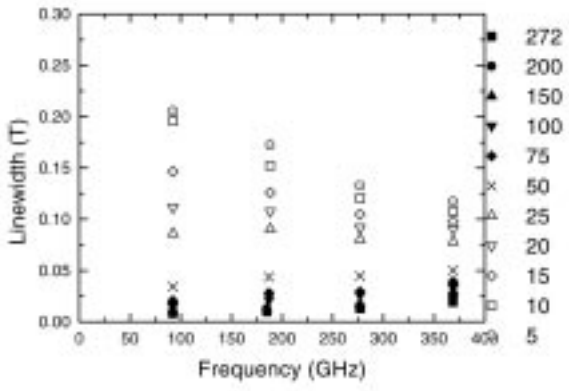

Figure 1. Linewidth vs. frequency for $Cd_{.7}Mn_{.3}S$.

For $Cd_{1-x}Mn_xSe$, alloys with Mn concentrations x = .2, .3, .4, .45 have been studied, and for $Cd_{1-x}Mn_xS$, the concentrations x = .2, .3, .4 have been investigated. For Mn^{2+} concentrations greater than .2, we have found that at low temperatures (less than 50 K), the linewidth decreases with increasing frequency, but at high temperatures, the linewidth increases with increasing frequency. For x = .2, however, the linewidth increases with increasing frequency for all temperatures, but this increase is greater for the lower temperatures. As the concentration decreases, the temperature at which the trend in linewidth dependence on frequency changes from increasing to decreasing also decreases, and it is apparent that at x = .2 we have not reached a temperature low enough to see the decrease in linewidth with increasing frequency. In summary, we have shown that in alloys whose concentrations are greater than .2, there are two temperature regimes for the linewidth dependence on the frequency, and that, in the temperature range explored so far (300 K to 5 K), a second mechanism dominates the linewidth when x = .2.

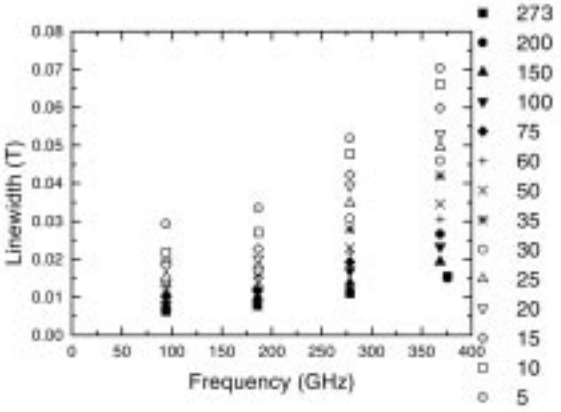

Figure 2. Linewidth vs. frequency for $Cd_{.8}Mn_{.2}S$.

References:

1 Moriya, T., Phys. Rev., 120, 91 (1960).

2 Larson, B.E., *et al.*, Solid State Commun., 56, 347 (1985).

Spectroscopic Studies of Quantum Limit Materials in a Magnetic Field

Musfeldt, J.L., State Univ. of New York (SUNY)-Binghamton, Chemistry

Wang, Y.J., NHMFL

Wei, X., NHMFL

Zhu, Z., SUNY-Binghamton, Chemistry

Long, V.C., SUNY-Binghamton, Chemistry

η-Mo_4O_{11} is a two-dimensional material which has been of sustained interest as a model charge density wave (CDW) compound, with incommensurate CDW transitions at 109 and 35 K, respectively.[1,2] More recently, η-Mo_4O_{11} has attracted attention as a prototypical quantum limit material.[3,4] Here, application of a magnetic field induces a semimetal $\rightarrow$ semiconductor transition, in which a gap opens up above the 20 T transition field. In this high-field regime, the magnetic energy is of the same order of magnitude as the electronic energy. Despite strong interest in this material from the transport community, a complimentary spectroscopic investigation has been lagging.

In order to investigate the nature of the quantum limit transition and behavior on passing through the various quantum Hall phases, we have made far-infrared and optical reflectance measurements of η-Mo_4O_{11} as a function of temperature and applied magnetic field. Our goal is to characterize the microscopic nature of these competing broken symmetry ground states.

Our first set of experiments explored the unpolarized far-infrared response (30-600 cm^{-1}) of η-Mo_4O_{11} up to 17 T in the superconducting magnet. Typical data is shown in Figure 1.[5] The main features of the reflectance ratio spectra include the change in curvature near 120 cm^{-1} and the overall drop starting near 60 or 70 cm^{-1}. When these reflectance ratio data are combined with absolute low-temperature power reflectance spectra, we can perform a Kramers-Kronig analysis

to calculate the optical constants of the material. This calculation shows that the drop in the far-infrared reflectance ratio translates into an increasingly prominent CDW_2 gap near 80 cm^{-1} with applied magnetic field.

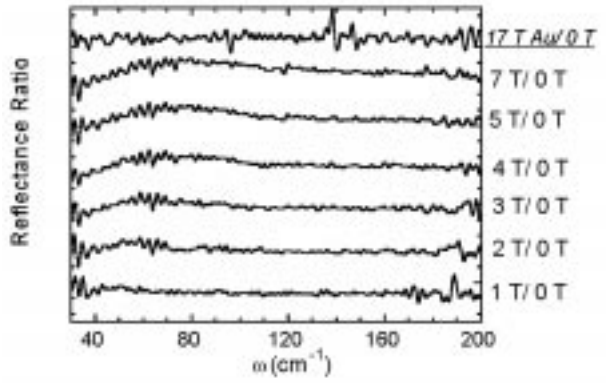

Figure 1. Ratio of reflectance at high magnetic field to the zero field reflectance at 4 K in the far-infrared.

More recently, a second set of experiments explored the polarized optical response (6000-40000 cm^{-1}) of η-Mo_4O_{11} as a function of magnetic field. These measurements were carried out in the 33 T resistive magnet, allowing us to pass through the series of low-field quantum Hall states as well as the 20 T semimetal $\rightarrow$ semiconductor Landau transition. Preliminary results suggest a redistribution of oscillator strength in several regimes on passing through the 20 T transition. A detailed analysis of these structures is currently in progress.

References:

1 Canadell, E., *et al*., Inorg. Chem., 28, 1466 (1989).
2 Guyot, H., *et al*., J. Phys. C: Sol. State. Phys., 16, L1227 (1983).
3 Sasaki, M., *et al*., Phys. Rev. B., 55, 4983 (1997).
4 Hill, S., *et al*., Phys. Rev. B., 58, 10772, (1998).
5 Zhu, Z., *et al*., Proceedings of the Physical Phenomena at High Magnetic Fields III Conference, submitted.

Demagnetization Versus Short Range Order Effects in Low-Dimensional Magnetic Materials: High Field EPR and Magnetization Measurements

Pardi, L.A., NHMFL, and Consorzio INSTM-Italy
Hassan, A.K., NHMFL
Hall, D., NHMFL
Brunel, L.-C., NHMFL
Gatteschi, D., Univ. of Florence-Italy, Chemistry
Caneschi, A., Univ. of Florence-Italy, Chemistry

This is the continuation of a project started with a high field-high frequency EPR investigation of a series of linear chain complexes made up by Gd(III) ions bridged by nitronyl-nitroxide organic radicals. Marked g-shifts were observed in the powder spectra of these materials, which were attributed to short range order (SRO) effects. The EPR experiments on these insulators are performed in the so-called depolarization regime, in which the static and the oscillating magnetic fields totally penetrate the sample. In this condition, the effective field acting on the EPR active center is different from the applied field (H), $B = H + 4\pi M$. The magnetization (M), in turn, contains contributions coming from different effects, one of them being the *demagnetization* or *shape effect*. This effect is also the cause of marked g-shifts in magnetic resonance, and needs to be taken into account when quantitatively assessing the size of any observed g-shifts. In the case of the Gd linear chain system we are considering, the effect is expected to be very different for the different samples because they show different behaviors of the magnetization vs. field curve. In order to assess the relevance of the demagnetization effects, we performed magnetization measurements with a SQUID up to 7 T, and with the vibrating sample magnetometer (VSM) at the NHMFL up to 33 T, on one of the linear chain systems: $Gd(hfac)_3NITEt$ (hfac = hexafluoro acetylacetonate, NITEt = 2-ethyl-4,4,5,5-tetramethyl-4,5-dihydro-1H-imidazolyl-1-

oxyl 3-oxide). The results are shown in Figure 1 as a magnetization vs. field plot at different temperatures. The system saturates slowly compared with the other systems in the series, namely $Gd(hfac)_3NITMe$, and $Gd(hfac)_3NITiPr$ (NITMe = 2-methyl-4,4,5,5-tetramethyl-4,5-dihydro-1H-imidazolyl-1-oxyl 3-oxide, NITiPr = 2-*iso*-propyl-4,4,5,5-tetramethyl-4,5-dihydro-1H-imidazolyl-1-oxyl 3-oxide). At the lowest temperature, 4 K, the magnetization of $Gd(hfac)_3NITEt$ reaches the value of 7.6 B.M. (which is close to the expected saturation value of 8 B.M.) only at the highest field (33 T). For the NITMe derivative the magnetization saturates at about 3 T at 1.7 K. From these results the internal field of the sample could be evaluated from:

$$H_i = H - NM$$

where H is the applied field, N is the demagnetizing tensor, and M is the volume magnetization of the sample. From the observed M we could calculate H_i for a series of sample shapes: disk, needle, sphere, and in the general case of an ellipsoid. In all cases, the internal field is of the order of few tens of mT, while the observed g-shifts in EPR are of the order of 1 T. The observed g-shifts cannot, thus, be attributed to demagnetization effects, confirming, therefore, the original hypothesis on their origin, i.e. SRO effects.

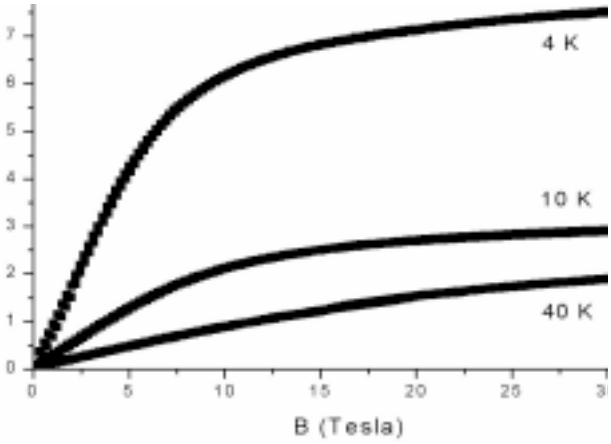

Figure 1. Magnetization measurements, at different temperatures, of $Gd(hfac)_3NITEt$ (hfac = hexafluoro acetylacetonate, NITEt = 2-ethyl-4,4,5,5-tetramethyl-4,5-dihydro-1H-imidazolyl-1-oxyl 3-oxide).

Determination of the Single Ion Anisotropy of Fe(III) in Large Magnetic Clusters

Pardi, L.A., NHMFL and Consorzio INSTM-Italy
Hassan, A.K., NHMFL
Brunel, L.-C., NHMFL
Cornia, A., Univ. of Modena-Italy, Chemistry
Gatteschi, D., Univ. of Florence-Italy, Chemistry
Sessoli, R., Univ. of Florence-Italy, Chemistry

Large magnetic clusters of metal ions are the focus of an intense activity in many branches of science, ranging from biology to condensed matter. The determination of the magnetic properties of this class of materials is a special case of interdisciplinary research. In particular, high nuclearity manganese and iron clusters are interesting for the synthesis of high spin molecules. High spin molecules in turn, having also a large Ising-type magnetic anisotropy, are of special interest as superparamagnetic particles. The source of magnetic anisotropy is thus very important in this contest. Magnetic anisotropy in exchange coupled systems has three main sources: single ion anisotropy, dipolar interaction, and exchange anisotropy. When the number of exchange coupled centers is large and when the symmetry of the system is low, it may be difficult to estimate the different contributions.

A series of β-diketonate alkoxide iron(III) complexes were synthesized including clusters having nuclearity ranging from 2 to 6. In all of these systems, antiferromagnetic coupling is observed between the iron ions. In the analysis of the magnetic properties of these systems, the single ion anisotropy can not be directly estimated for the reasons already mentioned. In order to access this piece of information, an isostructural dimer of Ga(III) was synthesized and doped with 5% of Fe(III). The hope was to observe the isolated Fe(III) ions in the same environment they are in the clusters, and thus directly measure the single ion anisotropy of Fe(III) by high field/frequency EPR.

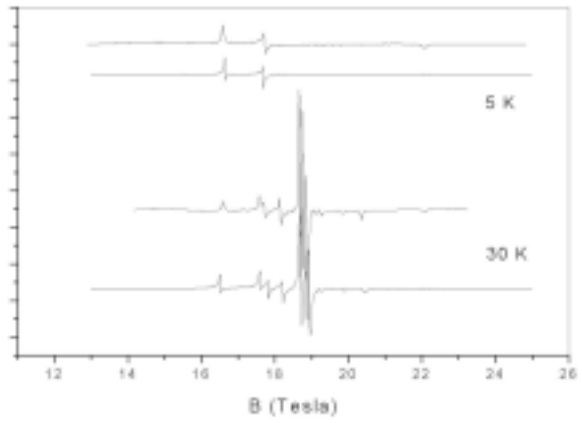

Figure 1. EPR spectra at 525 GHz of $Ga_{1-x}Fe_x(OCH_3)_2$ (dbm) at 30 K and 5 K. Upper trace: experimental. Lower trace: simulated spectra.

The EPR spectra of a sample of $Ga_{1-x}Fe_x(OCH_3)_2(dbm)_4$ (dbm = dibenzoylmethanate) with x = 0.05 ca were recorded at frequencies ranging from 110 GHz to 525 GHz using the EMR facility at the NHMFL. The spectra at 525 GHz are shown in Figure 1 for two different temperatures. The spectra were recorded using a CO_2 pumped FIR laser as a source, and a resistive magnet (the Keck magnet) operative in cell 6 at the NHMFL. Fits of the spectra, also shown in Figure 1, gave the zero field splitting parameters D = 0.77 cm^{-1} and E/D = 0.1, and an isotropic g equal to 2 for a S = 5/2. The success of this experiment, showing the high sensitivity of the EPR spectrometer allowing to work with low concentrations, prompted us to start a project of characterization of Iron doped Ga(III) clusters.

High Field/High Frequency EPR Investigation of Transition Metal Ion Adducts with Semiquinones

Pardi, L.A., NHMFL and Consorzio INSTM-Italy
Hassan, A.K., NHMFL
Brunel, L.-C., NHMFL
Gatteschi, D., Univ. of Florence-Italy, Chemistry
Dei, A., Univ. of Florence- Italy, Chemistry

In the continuing effort to characterize the magnetic properties of quinonoid adducts with transition metal ions, we used HF-EPR spectroscopy in order to determine the charge distribution and the nature of the ground state of this class of compounds. Quinonoid molecules are present in a number of systems, in which, their valence is unequivocally determined either by simple charge balance or by X-ray structure determination. The complex: $[Ni(CTH)DTBSQ]PF_6$ (CTH = *dl*-5,7,7, 12,14,14-hexamethyl- 1,4,8,11 - tetrazacyclo-tetradecane, DTBSQ = 3,5 - di - *tert* - butylsemi-quinone) has an S = 3/2 ground state originating from the ferromagnetic coupling between the S = 1 Ni(II) ion and the S = 1/2 SQ radical confirmed by magnetic measurements and molecular structure. In the complex $[Ni(TCdiox)_2N_3]$, (TCdiox = Tetrachloro dioxolene and N_3 = 2,2,4-trimethyl-1,5,9-triaza-cyclododec -1-ene), the charge distribution in the system can be such that it can be formulated either as $[Ni^I(TCQ)(TCSQ)N_3]$ (TCQ = Tetrachloro-Quinone, TCSQ = Tetrachloro-Semiquinone) or as $[Ni^{II}(TCCat)(TCQ)N_3]$ (TCCat = Tetrachloro-Cathecolate). The first formulation seems more appropriate on the basis of the structural features. In both cases, the system is expected to have an S = 1 ground state that is consistent with the observed magnetic properties. In the first case, this triplet state would be the result of a strong ferromagnetic interaction between the S = 1/2 Ni^I and the S = 1/2 SQ. In the second case, the Ni^{II} ion with its two unpaired electrons generates the S = 1 state. In the two cases, the magnetic properties would be very similar, but the EPR properties are different. In $[Ni^I(TCQ)(TCSQ)N_3]$, the g tensor would be the average of the g tensors of the two S = 1/2 paramagnetic centers, namely the Ni(I) (d^9) and the SQ radical. Therefore, a g tensor with principal values close to the free electron value is expected. In the case of $[Ni^{II}(TCCat)(TCQ)N_3]$, the g tensor would be that of the Ni(II) ion, which with its sizeable spin orbit coupling (ξ = 300 cm^{-1}) generally shows a marked anisotropy with g values different from 2.0. Moreover, all of these systems show large zero field splitting (zfs), and thus HF-EPR spectroscopy is very well adapted to answer the question of the nature of the ground state.

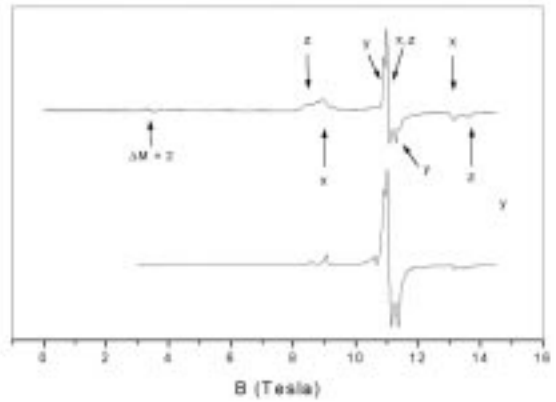

Figure 1. EPR spectra at 330 GHz and 4 K of [Ni(CTH)DTBSQ]PF_6. Upper trace: experimental. Lower trace: simulation.

In Figure 1, we show the spectrum of [Ni(CTH)DTBSQ]PF_6 at 330 GHz and 4 K. This spectrum is interpreted as the spectrum of an S = 3/2 state with a rhombic zfs: D = 1.2 cm^{-1}, E/D = 0.218 and g_x = 2.10, g_y = 2.11 and g_z = 2.12. In Figure 2, we show the multifrequency spectra of [Ni(TCdiox)$_2N_3$ at 10 K. In this case, the possibility to perform spectra with a variety of frequencies, up to 525 GHz, was essential for the understanding of the problem. The observed spectra could be fitted with a D = 3 cm^{-1}, and a large rhombic distortion (E/D = 1/3 ca) for g = 2.2. Therefore, the complex has to be formulated as [Ni^{II}(TCCat)(TCQ)N_3]. On the basis of structural data, the formulation was instead [Ni^{I}(TCQ)(TCSQ)N_3]. Thus, a conflict between the spectroscopic and the structural determination is raised. It is interesting to note that up to now the structural criteria has been very often used for the assessment of charge distribution in quinonoid complexes of transition metal ions.

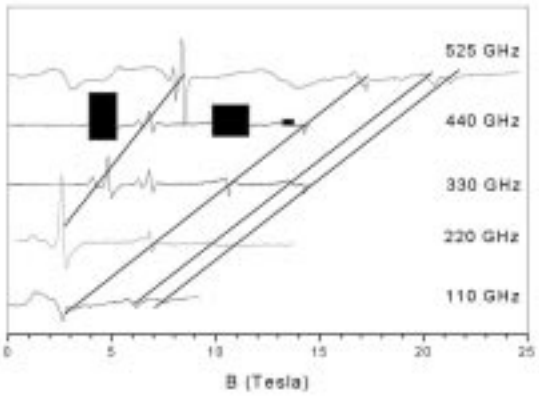

Figure 2. Multifrequency EPR spectra of [Ni(TC diox)$_2N_3$] at 10 K.

Glassy Behavior of Random Field Magnets

Pastor, A.A., NHMFL/FSU, Physics
Dobrosavljevic, V., NHMFL/FSU, Physics

The key unresolved feature of the random field Ising model is the complex, history dependent behavior found both in experiments and numerical simulations. It appears that for strong enough disorder, and low temperatures, the system falls out of equilibrium, displaying anomalously slow relaxation and other features characteristic of glassy materials. Recently, it has been proposed that this behavior reflects the emergence of a low temperature glassy phase, which can be mathematically described as a replica symmetry breaking instability.

In this study, we use a 1/z expansion approach (z is the coordination number), and examine the glassy behavior of the random-field Ising model. The random field Ising model (RFIM) is one of the simplest models of disordered interacting systems. It is believed to describe the behavior of diluted antiferromagnets in strong magnetic fields, but it is also likely to be crucial for understanding some aspects of the metal-insulator transition in disordered electronic systems . In recent years, there have been many theoretical[1] and experimental[2] indications that the essential difficulties in unraveling the behavior of the RFIM may be related to the existence of many metastable states and the associated glassy phase, similar to those found in spin glass materials . Standard approaches, such as the Bragg-Williams mean field theory (MFT), when used to examine the RFIM, predicted only the existence of the ferromagnetic (FM) and the paramagnetic (PM) phases, but failed to identify a spin-glass (SG) phase. Very recently, by including fluctuations beyond MFT using a 1/N approach, Mezard and Young[1] were successful in predicting the SG phase, based on an appropriate replica symmetry breaking scheme. However, this formulation is fairly complicated, making it

difficult to obtain simple analytical results, or to extend the theory to more complex situations.

In this work, we propose an approach[3] based on a 1/z expansion (z is the coordination number), that is technically simpler and more convenient for generalizations, but reduces to standard MFT for large z. Our approach is to be able to identify an SG phase, and allow us to study its properties for high disorder. This method would be easier to extend to quantum mechanical models than the 1/N approaches, and thus, may be useful for the study of metal-insulator transitions in disordered electronic systems.

References:

1 Mezard, M., *et al*., Europhys. Lett., 18, 653 (1992).
2 Montenegro, F.C., *et al*., Phys. Rev. B., 44, 2155 (1991).
3 Pastor, A.A., *et al*., proc. of Physical Phenomena at High Magnetic Fields-III.

Comparison of Cl_2/He, Cl_2/Ar and Cl_2/Xe Plasma Chemistries for Dry Etching of NiFe and NiFeCo

Pearton, S.J., UF, Materials Science and Engineering (MSE)/NHMFL
Sharifi, F., UF, Physics/NHMFL
Jung, K.B., UF, MSE

Currently most patterning of magnetic multilayer structures used for thin film read/write heads and magnetic random access memories is performed with Ar^+ ion milling processes, where the material is sputtered away by physical momentum transfer. It is likely that this process will be acceptable for several more generations of device design, but for very small feature sizes, ion milling suffers from two drawbacks. The first is that there is little selectivity to all mask materials, so that sloped sidewalls will result from mask faceting, limiting the ultimate feature size possible. The second is that redeposition on the feature sidewalls might affect the magnetic switching characteristics.[1] For these reasons, it is desirable to develop alternative pattern transfer processes. One option is an etch process with a chemical component in addition to a physical component. It is clearly possible to heat the sample during plasma etching in order to enhance the volatility of the etch products, but magnetic multilayer structures have limited thermal stability against interdiffusion. We have previously reported that high density plasma reactors are capable of etching NiFe and NiFeCo at practical rates using Cl_2/Ar discharges. The high ion flux in these systems appears to prevent formation of the selvedge or reaction layer of involatile chlorides on the surface of the magnetic materials that occurs in conventional reactive ion etch systems. The role of the inert gas additive to the Cl_2 is important in providing much of the ion-assisted desorption of the chloride etch products, but to date there has been no systematic study of the effect of using different species.

A comparison was performed of He, Ar, and Xe as additives to Cl_2 Inductively Coupled Plasmas (ICP) for etching of thin film NiFe and NiFeCo. The rf chuck power (controlling incident ion energy), source power (controlling ion flux) and plasma composition have been varied to see their effect on etch rates, while the near-surface stoichiometry has been examined by Auger Electron Spectroscopy (AES).

Layers of $Ni_{0.8}Fe_{0.2}$, $Ni_{0.8}Fe_{0.13}Co_{0.07}$, Ni, and Fe in the thickness range of 3000 Å to 5000 Å were deposited on Si by dc magnetron sputtering. For etch rate experiments the samples were masked with Apiezon wax, which was later removed in trichloroethylene and the etch depth measured by stylus profilometry. Dry etching was performed in a Plasma Therm 790 ICP system, in which the sample sits on an 8"ϕ, rf-biased (13.56 MHz), He-backside cooled electrode. The rf power was varied from 50 W to 350 W, and this controls the dc self-bias on the electrode at a given source power. The plasma is generated by application of 2 MHz rf power (0 to 1000) to the ICP source, using a 3-turn coil that is closely coupled (4 cm plasma-sample distance) to the sample electrode. The

process pressure was held constant at 5 m Torr, with a total gas load of 15 standard cubic centimeters per minute (sccm).

The role of the inert gas additive during Cl_2-based ICP etching of NiFe and NiFeCo thin films was investigated as a function of source power, rf chuck power and plasma composition. All three additives investigated, He, Ar, and Xe, provide effective etching of these materials provided the ion energy and flux are above particular thresholds. The etch rates are higher for the heavier species due to their increased sputtering efficiency, but smoother etched surfaces were obtained for Cl_2/He plasmas. A key focus of future work should be in trying to determine the extent of any ion-induced damage to feature sidewalls that would affect the magnetic switching characteristics. It has been found in ion-milled magnetic memory elements that high ion energies (1000 V) leads to a reduction in coercivity in pseudo spin bit arrays of a factor of eight relative to elements fabricated with low ion energies (300 V). The etch yields with the Cl_2-based processes are still low (typically ~ 0.1 atoms of the magnetic material removed per incident ion), emphasizing that a high ion flux is crucial.

Reference:

1 Jung, K.B., *et al.*, J. Vac. Sci. Technol., A16, 1697 (1998).

Iodine- and Bromine-Based Dry Etching of $LaCaMnO_3$

Pearton, S.J., UF, Materials Science and Engineering (MSE)/NHMFL
Sharifi, F., UF, Physics/NHMFL
Dahmen, K.H., FSU, MARTECH
Cadieu, F., Queens College of New York, Physics
Wang, J.J., UF, MSE

Lanthanum manganite perovskite materials exhibiting a large magnetic field-induced resistivity transition are attracting interest for possible application in new generations of magnetic memories and sensors. The utility of these colossal magnetoresistive (CMR) materials will depend on a number of factors, including the ability to provide a sufficiently high field (typically ≥ 1 T) at the magnetic element to observe the CMR effect. A general problem when processing magnetoresistive materials is their relative involatility in conventional dry etch techniques such as Reactive Ion Etching (RIE). For this reason read/write heads and other structures are patterned by ion beam etching, which typically exhibits little selectivity over the masking material and can lead to substantial redeposition on the sidewall of etched features. While a degree of chemical etch enhancement can be obtained for NiFe and NiFeCo using Cl_2-based plasmas under high ion density conditions, previous work on $La_xCa_{1-x}MnO_3$ has shown there is no chemical enhancement in etch rate over simple Ar sputtering for Cl_2, SF_6 or CH_4/H_2 plasma.

We studied use of two novel plasma chemistries, BI_3 and BBr_3, for dry etching of $LaCaMnO_3$. We observe a small degree of chemical enhancement with both chemistries at low halide composition (20% to 40% by flow) in the discharges. The etching is still strongly dependent on ion energy and flux, and is highly anisotropic.

Liquid delivery metalorganic chemical vapor deposition using 2,2,6,6-tetramethyl-3, 5-heptanedionato (TMHD) precursors (i.e. $La(TMHD)_3$, $Sr(TMHD)_2$, $Mn(TMHD)_3$ and $Ca(TMHD)_2$) was employed to deposit films of $La_{0.41}Ca_{0.59}MnO_3$ on Al_2O_3 (0001) single crystal substrates at 700 °C. The precursors were transported by N_2 carrier gas, with direct injection of O_2 and N_2O as oxidants.

Samples were patterned with either Apiezon wax for etch rate measurements or with plasma-enhanced chemical vapor deposited SiO_2 for examination of the anisotropy of the etching. The etching was performed in a Plasma-Therm 790 reactor in which the plasma is generated by a 3-turn inductive coil operated with up to 1000 W of 2 MHz power. The sample position was separately powered with 0 W to 450 W of 13.56 MHz power. This chuck is He backside-cooled to

hold the sample temperature to ≤ 40 °C. Process pressure was held constant at 5 m Torr for all experiments. The BI_3 (melting point 40 °C) and BBr_3 (boiling point 91 °C) were held at ~ 45 °C within a stainless steel vacuum vessel; total gas loads of 10 standard cubic centimeters per minute (sccm) were injected into the Inductively Coupled Plasma (ICP) source through electronic mass flow controllers. Etch rates were determined by stylus profilometry measurements using a Tencor system after removal of the mask material. Surface morphologies were examined with Scanning Electron Microscopy (SEM) and Atomic Force Microscope (AFM) using a Si tip in tapping mode.

Excellent pattern transfer was achieved with both chemistries, with the ability to make sub-micron features demonstrated. Previous work with plasma chemistries based on Cl_2, F_2 or CH_4/H_2 did not show any degree of chemical enhancement for etching of $LaCaMnO_3$.[1] Use of I_2- or Br_2-based mixtures provides a small degree of chemical enhancement relative to pure Ar sputtering, and enables smooth, anisotropic pattern transfer. The etch rates are a strong function of plasma composition, ion flux and ion energy. Calculated ion-to-neutral ratios on order 0.02 are available under ICP conditions (much higher than in conventional RIE tools, ~ 10^{-6}), and provide the ability to enhance the desorption of otherwise involatile etch products. However it is still problematic as to whether there is sufficient advantage gained by using BI_3 and BBr_3 relative to pure Ar sputtering to justify the extra precautions needed in handling these corrosive materials.

Reference:

1 Wang, J.J., *et al*., J. Electrochem. Soc., 145, 2512 (1998).

Relative Merits of Cl_2 and CO/NH_3 Plasma Chemistries for Dry Etching of MRAM Device Elements

Pearton, S.J., UF, Materials Science and Engineering (MSE)/NHMFL
Sharifi, F., UF, Physics/NHMFL
Jung, K.B., UF, MSE
Cho, H., UF, MSE

Magnetic Random Access Memories (MRAM) offer high storage densities, fast access time, radiation hardness and infinite re-write capability. Current element sizes are on order 2 μm, but there is a strong trend toward sub-micron geometries to increase bit storage density. The standard method for patterning the magnetic multilayers that comprise the memories is ion milling, which has some potential drawbacks such as sidewall redeposition and lack of selectivity between different materials. Conventional reactive ion etching (RIE) works only at temperatures (> 300 °C) in excess of the thermal stability of these multilayers.[1]

Recently we have found that high ion density plasma reactors such as Electron Cyclotron Resonance (ECR) and Inductively Coupled Plasma (ICP) can effectively etch magnetic multilayers using a Cl_2/Ar chemistry. The etch mechanism involves the reaction of a thin chlorinated surface layer, which is removed by ion-assistance before it can build into a non-volatile selvedge region (as occurs in RIE). The key difference that occurs with high density conditions is the high ion flux balances the formation and removal of the chlorinated etch product layer. Potential drawbacks with this chemistry include corrosion of the magnetic materials from residue chlorine.

In this report we compare the Cl_2-based plasma chemistry with the CO/NH_3 mixture. The latter has been reported to produce low (350 Å·min^{-1}) rates for $Ni_{0.8}Co_{0.045}Fe_{0.155}$ in a magnetron-type reactor.

5000 Å thick layers of $Ni_{0.8}Fe_{0.2}$ and $Ni_{0.8}Fe_{0.13}Co_{0.07}$ were deposited by dc magnetron sputtering on SiO_2-coated Si wafers. Masks of either photoresist or bias-sputtered SiO_2 were employed. Dry etching was performed in a Plasma Therm 790 reactor, comprising a 2 MHz, 3-turn ICP source power (1500 W) and a He backside-cooled, rf powered (13.56 MHz, 450 W) sample chuck. Two different plasma chemistries were investigated: Cl_2, with additions of either Ar, N_2, or H_2, and CO/NH_3. The etch products in the former case are expected to be chlorides (e.g. $NiCl_X$), which in the latter case, they should be carbonyls (e.g. $Ni(CO_4)$). Etch rates were obtained from stylus profilometry measurements, while etch anisotropy was examined from scanning electron microscopy (SEM).

Etch rates were typically up to 1000 Å·min^{-1} with Cl_2, but a factor of three lower with CO/NH_3. The CO/NH_3 plasma chemistry appears promising for shallow, corrosive-free etching of NiFe and NiFeCo. It is still a physically-dominated chemistry, so that mask erosion can be prohibitive for deep etching. Photoresist cannot be used as a mask, but SiO_2 is stable for shallow etching. This chemistry still requires a high density reactor to produce practical etch rates. By comparison, Cl_2-based chemistries produce high rates due to a stronger chemical component, and hence there is less mask erosion. Post-etch cleaning is critical for avoiding corrosion with these latter chemistries.

Reference:

1 Jung, K.B., *et al*., Appl. Phys. Lett., 71, 1255 (1997).

High Field EPR of High-Spin Polynuclear Manganese Compounds

Ruiz, D., Univ. of California-San Diego, Chemistry
Hassan, A.K., NHMFL
Maniero, A.L., NHMFL
Christou, G., Indiana Univ., Chemistry
Brunel, L.-C., NHMFL
Hendrickson, D.N., Univ. of California-San Diego, Chemistry

Complexes of the composition $[Mn_{12}O_{12}(O_2CR)_{16}(H_2O)_4]$ (called Mn_{12}) have attracted considerable attention in the last few years.[1,2] As a result of a large spin ground state and significant magnetoanisotropy, such complexes exhibit magnetization relaxation phenomena, such as a magnetization hysteresis loop. Therefore, Mn_{12} are suitable candidates to be used as high-density storage devices.

Two different kinds of magnetization relaxation processes have been found in Mn_{12} molecules. Some complexes exhibit an out-of-phase signal in the region 2 K to 4 K, while other complexes exhibit an out-of-phase signal in the region 4 K to 7 K. In order to understand the origin of these two different relaxation phenomena, high field EPR experiments can be conclusive. Unlike magnetic susceptibility measurements that are a bulky property reflecting Boltzman population of states, in an EPR experiment direct transitions between states are seen, and therefore, direct information about the energy barrier for the interconversion from the spins "up" to the spins "down" is obtained. We analyzed complexes showing both kinds of magnetization relaxation processes. First, Mn_{12} complexes showing slow magnetization relaxation rates were studied. In this order, high field EPR spectra of microcrystalline samples of complexes $[Mn_{12}O_{12}(O_2CR)_{16}(H_2O)_4]$ where R = $-CD_3$ and $-CH_2C_6H_5$ at a frequency of 328 GHz and

440 GHz, and temperatures between 4.5 K and 40 K, were obtained. In both cases, two or three peaks can be observed at low temperatures corresponding to the transitions of molecules from an ms level to an ms+1 level. For the spectra collected at higher temperatures incrementally more peaks grow in at higher fields because more ms to ms+1 transitions are possible as Boltzman thermal population of higher energy states increases. In the case of the deuterated sample, up to eleven peaks associated to eleven transitions from an ms to an ms+1 level can be observed. The single reduced form of the complex $[Mn_{12}O_{12}(O_2CR)_{16}(H_2O)_4]$, where R is p-fluorobenzoic acid, was also studied. Several peaks associated to transitions from an ms to an ms+1 level were also observed. Further analysis of the data is required to extract more information about the magnetic ground state, zero-field splitting and the g value of each complex.

HF-EPR spectra of microcrystalline samples of complexes showing faster relaxation rates were also studied. High field EPR spectra of complexes $[Mn_{12}O_{12}(O_2CR)_{16}(H_2O)_4]$, where R= $-FC_6H_4$ and $-C_6H_5(NO_2)_2$, were obtained. In this case, rather complicated spectra, even at very low temperatures (below 4.5 K), were obtained due to the fast magnetization relaxation rates that these complexes undergoes even at very low temperatures. Again, the microcrystals were not restrained thus allowing them to torque in field. At low temperatures, several peaks in the low-field and high-field regions were detected. As the temperature is raised one expects that new peaks of the different transitions will become evident since more transitions are possible due to the increased Boltzman population of higher energy states. However, not only the peaks observed at low fields disappear at high temperature, but surprisingly, the intensity of the peaks observed at high fields increase. These data are under investigation.

References:

1 Aubin, S.M.J., *et al*., submitted to J.A.C.S.

2 Barra, A.L., *et al*., Accounts of Chemical Research, 31, 460 (1998).

Numerical Calculations of the B_{1g} Raman Spectrum of the Two-Dimensional Heisenberg Model

Sandvik, A., NHMFL

Dagotto, E., NHMFL/FSU, Physics and MARTECH

Capponi, S., Lab. de Physique Quantique, Univ. Paul Sabatier, Toulouse, France

Poilblanc, D., Lab. de Physique Quantique, Univ. Paul Sabatier, Toulouse, France

The B_{1g} Raman spectrum of the two-dimensional S = 1/2 Heisenberg model is discussed within the Loudon-Fleury theory at both zero and finite temperatures.[1] The exact T = 0 spectrum for lattices with up to 6 x 6 sites is computed using Lanczos exact diagonalization. A quantum Monte Carlo (QMC) method is used to calculate the corresponding imaginary-time correlation function, and its first two derivatives for lattices with up to 16 x 16 spins. The imaginary time data is continued to real frequency using the maximum entropy method, as well as a fit based on spinwave theory. The numerical results are compared with spinwave calculations for finite lattices. There is a surprisingly large change in the exact spectrum going from 4 x 4 to 6 x 6 sites. In the former case there is a single dominant two-magnon peak at $\omega/J \approx 3.0$, whereas in the latter case there are two approximately equal sized peaks at $\omega/J \approx 2.7$ and 3.9. This is in good qualitative agreement with the spinwave calculations including two-magnon processes on the same lattices. The spinwave results for larger lattices show how additional peaks emerge with increasing lattice size, and eventually develop into the well known two-magnon profile peaked at $\omega/J \approx 3.2$, and with weight extending up to $\omega/J \approx 4.6$. Both the Lanczos and the QMC results indicate that the actual two-magnon profile is broader than the narrow peak obtained in spinwave theory, but the positions of the maxima agree to within a few percent. The higher-order contributions present in the numerical results are merged with the two-magnon profile, and extend

up to frequencies $\omega/J \approx 7$. The first three frequency cumulants of the spectrum are in excellent agreement with results previously obtained from a series expansion around the Ising limit. Typical experimental B_{1g} spectra for La_2CuO_4 are only slightly broader than what we obtain here. The exchange constant extracted from the peak position is $J \approx 1400$ K, in good agreement with values obtained from neutron scattering and NMR experiments. We discuss the implications of our present results for more sophisticated theories of Raman scattering suggested recently.

Reference:

1 Sandvik, A., *et al*., Phys. Rev. B, 57, 8478 (1998).

Magnetoresistance Measurements on RAlSi Compounds

Sarrao, J.L., LANL
Petrovic, C.N., LANL/FSU, Physics
Lacerda, A.H., NHMFL/LANL
Hundley, M.F., LANL
Thompson, J.D., LANL
Fisk, Z., NHMFL/FSU, Physics

We have recently synthesized single crystals of RAlSi (where R is a light rare-earth, e.g. Ce or Gd) that form in an ordered variant of the α-$ThSi_2$ structure. In addition to displaying a low carrier density, these materials order magnetically at low temperature, with an ordering temperature that varies with the rare earth ion. For some R, e.g. Nd and Sm, multiple magnetic transitions are observed in zero-field specific heat and low-field magnetic susceptibility measurements. We have performed magnetoresistance measurements on GdAlSi for $4\ K < T < 100\ K$ and $0 < B < 18$ T using the 20 T superconducting magnet at the NHMFL-Los Alamos Pulsed Field Facility. We find that as a function of increasing field, the magnetic transition that occurs near 30 K in zero field splits into a series of transitions between 20 K and 40 K by 18 T. Although further work is required to sort out the details of these transitions, including performing high-field magnetization measurements, it would appear that the metamagnetic transitions induced by field in GdAlSi are similar to the multiple zero-field transitions in NdAlSi and SmAlSi, and are due to reorientation of the rare-earth spin.

High Magnetic Field Properties of $CeRh_3B_2$

Torikachvili, M.S., San Diego State Univ., Physics
Huber, J.G., NHMFL/LANL
Lawson, A.C., NHMFL/LANL
Schmiedeshoff, G.M., Occidental College, Physics

The compound $CeRh_3B_2$ displays ferromagnetic (FM) order below $T_c \approx 115$ K.[1] Several mechanisms have been proposed to explain this unusually high T_c for a Ce compound. Dhar, *et al*., suggested that the magnetism was itinerant, and probably associated with the 4d- electrons of the Rh. This conjecture, however, is not supported by other findings. For example, (1) neighboring isotype $LaRh_3B_2$ is not FM, and (2) resonant photoemission reveals that the density of Rh-4d states at the Fermi level is too small to

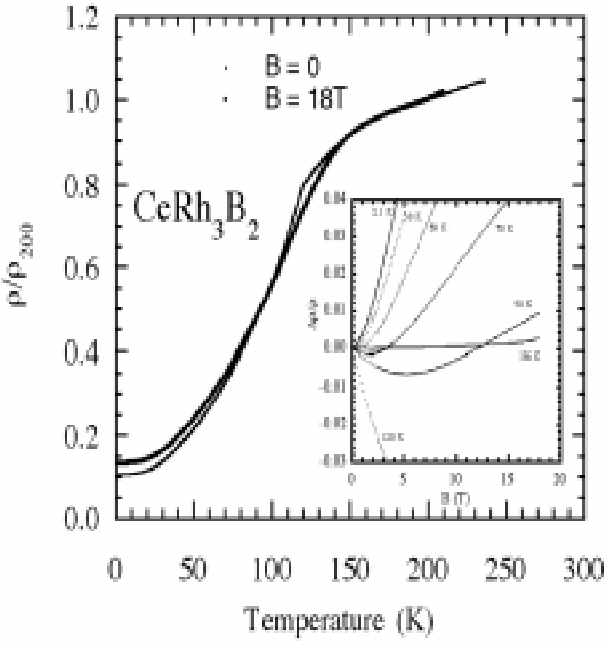

Figure 1. Normalized ρ/ρ_{200K} vs. T in B = 0 and 18 T. The inset shows plots of $\Delta\rho/\rho$ vs. B.

support itinerant FM. Muon-spin relaxation experiments, however, show that the local field increases in magnitude below T_c. It reaches a maximum value of 13 mT at ≈ 50 K, and then drops to 11 mT at 12 K.[1] The reduction of the local field below 50 K suggests ordering of the Rh moments, oriented antiferrimagnetically with respect to the Ce moments.[2]

In order to probe further the magnetism in $CeRh_3B_2$, we performed measurements of magnetoresistance (MR) and magnetization in the 2 – 300 K temperature range, in B ≤ 20 T. The isofield curves of normalized resistivity, $\rho/\rho_{200K,}$ are displayed in Figure 1. The zero-field data shows a break in ρ vs. T suggesting that the onset of the FM transition occurs at ≈ 120 K. The MR is very small and positive well above T_c, then it becomes negative close to T_c, reflecting the suppression of magnetic scattering. In the 70 to 90 K range the MR is first negative, goes through a minimum, and then becomes positive in higher B. The minimum in MR below T_c moves to lower B at lower T. Below 50 K the MR is always positive, reaching ≈ 24% at 2 K in B = 18 T. The behavior of the MR in the low T range is typical of a metal, and it does not show any obvious features that could be associated with the onset of magnetic order in the Rh sublattice.

References:

1 Dhar, S.K., *et al.*, J. Phys. C, 14, L-321 (1981).
2 Cooke, D.W., *et al.*, Phil. Mag. B, 74, 259 (1996).

Antiferromagnetic Resonance in the Cubic Perovskite $KNiF_3$

NHMFL

Yamaguchi, H., The Institute of Physical and Chemical Research (RIKEN), Japan
Katsumata, K., RIKEN
Hagiwara, M., RIKEN
Tokunaga, M., RIKEN
Liu, H.L., UF, Physics
Zibold, A., UF, Physics
Tanner, D.B., UF, Physics/NHMFL
Wang, Y.J., NHMFL

Low temperature, high magnetic field, far infrared spectroscopy and electron spin resonance measurements have been performed on single crystals of the cubic perovskite $KNiF_3$. We found the absorption at 48.7 ± 0.3 cm^{-1} observed by Richards,[1] that was attributed to antiferromagnetic resonance (AFMR), is not magnetic in origin. Instead, a new absorption (at 2.5 cm^{-1} in zero field) is well fit by a theory[2] of AFMR with uniaxial anisotropy. Analysis yields an anisotropy energy of 8.7 x 10^{-3} cm^{-1}. The ratio between the anisotropy field and the exchange field is 2.4 x 10^{-5}. Thus, $KNiF_3$ is an excellent example of a Heisenberg antiferromagnet.

References:

1 Richards, P.L., J. Appl. Phys., 34, 1237 (1963).
2 Nagamiya, T., *et al.*, Adv. Phys., 4, 1 (1955).